NASA/TM—2018-219756

The Erosion of Diamond and Highly Oriented Pyrolytic Graphite After 1.5 Years of Space Exposure

Kim K. de Groh
Glenn Research Center, Cleveland, Ohio

Bruce A. Banks
Science Application International Corporation, Cleveland, Ohio

February 2018

NASA STI Program . . . in Profile

Since its founding, NASA has been dedicated to the advancement of aeronautics and space science. The NASA Scientific and Technical Information (STI) Program plays a key part in helping NASA maintain this important role.

The NASA STI Program operates under the auspices of the Agency Chief Information Officer. It collects, organizes, provides for archiving, and disseminates NASA's STI. The NASA STI Program provides access to the NASA Technical Report Server—Registered (NTRS Reg) and NASA Technical Report Server—Public (NTRS) thus providing one of the largest collections of aeronautical and space science STI in the world. Results are published in both non-NASA channels and by NASA in the NASA STI Report Series, which includes the following report types:

- TECHNICAL PUBLICATION. Reports of completed research or a major significant phase of research that present the results of NASA programs and include extensive data or theoretical analysis. Includes compilations of significant scientific and technical data and information deemed to be of continuing reference value. NASA counter-part of peer-reviewed formal professional papers, but has less stringent limitations on manuscript length and extent of graphic presentations.

- TECHNICAL MEMORANDUM. Scientific and technical findings that are preliminary or of specialized interest, e.g., "quick-release" reports, working papers, and bibliographies that contain minimal annotation. Does not contain extensive analysis.

- CONTRACTOR REPORT. Scientific and technical findings by NASA-sponsored contractors and grantees.

- CONFERENCE PUBLICATION. Collected papers from scientific and technical conferences, symposia, seminars, or other meetings sponsored or co-sponsored by NASA.

- SPECIAL PUBLICATION. Scientific, technical, or historical information from NASA programs, projects, and missions, often concerned with subjects having substantial public interest.

- TECHNICAL TRANSLATION. English-language translations of foreign scientific and technical material pertinent to NASA's mission.

For more information about the NASA STI program, see the following:

- Access the NASA STI program home page at http://www.sti.nasa.gov

- E-mail your question to help@sti.nasa.gov

- Fax your question to the NASA STI Information Desk at 757-864-6500

- Telephone the NASA STI Information Desk at 757-864-9658

- Write to:
  NASA STI Program
  Mail Stop 148
  NASA Langley Research Center
  Hampton, VA 23681-2199

NASA/TM—2018-219756

The Erosion of Diamond and Highly Oriented Pyrolytic Graphite After 1.5 Years of Space Exposure

Kim K. de Groh
Glenn Research Center, Cleveland, Ohio

Bruce A. Banks
Science Application International Corporation, Cleveland, Ohio

National Aeronautics and
Space Administration

Glenn Research Center
Cleveland, Ohio 44135

February 2018

Level of Review: This material has been technically reviewed by technical management.

Available from

NASA STI Program
Mail Stop 148
NASA Langley Research Center
Hampton, VA 23681-2199

National Technical Information Service
5285 Port Royal Road
Springfield, VA 22161
703-605-6000

This report is available in electronic form at http://www.sti.nasa.gov/ and http://ntrs.nasa.gov/

The Erosion of Diamond and Highly Oriented Pyrolytic Graphite After 1.5 Years of Space Exposure

Kim K. de Groh
National Aeronautics and Space Administration
Glenn Research Center
Cleveland, Ohio 44135

Bruce A. Banks
Science Application International Corporation
Cleveland, Ohio 44135

Abstract

Polymers and other oxidizable materials on the exterior of spacecraft in the low Earth orbit (LEO) space environment can be eroded due to reaction with atomic oxygen (AO). Therefore, in order to design durable spacecraft, it is important to know the LEO AO erosion yield (E_y, volume loss per incident oxygen atom) of materials susceptible to AO reaction. The Polymers Experiment was developed to determine the AO E_y of various polymers and other materials flown in ram and wake orientations in LEO. The experiment was flown as part of the Materials International Space Station Experiment 7 (MISSE 7) mission for 1.5 years on the exterior of the International Space Station (ISS). As part of the experiment, a sample containing Class 2A diamond (100 plane) and highly oriented pyrolytic graphite (HOPG, basal and edge planes) was exposed to ram AO and characterized for erosion. The materials were salt-sprayed prior to flight to provide isolated sites of AO protection. The E_y of the samples was determined through post-flight electron microscopy recession depth measurements. The experiment also included a Kapton H witness sample for AO fluence determination. This paper provides an overview of the MISSE 7 mission, a description of the flight experiment, the characterization techniques used, the mission AO fluence, and the LEO E_y results for diamond and HOPG (basal and edge planes). The data is compared to the E_y of pyrolytic graphite exposed to four years of space exposure as part of the MISSE 2 mission. The results indicate that diamond erodes, but with a very low E_y of $1.58 \pm 0.04 \times 10^{-26}$ cm^3/atom. The different HOPG planes displayed significantly different amounts of erosion from each other. The HOPG basal plane had an E_y of $1.05 \pm 0.08 \times 10^{-24}$ cm^3/atom while the edge plane had a lower E_y of only $5.38 \pm 0.90 \times 10^{-25}$ cm^3/atom. The E_y data from this ISS spaceflight experiment provides valuable information for understanding of chemistry and chemical structure dependent modeling of AO erosion.

Introduction

Materials used on the exterior of spacecraft are subjected to many environmental threats that can cause degradation. In low Earth orbit (LEO) these threats include photon radiation, ultraviolet (UV) radiation, vacuum ultraviolet (VUV) radiation, x-rays, solar wind particle radiation (electrons, protons), cosmic rays, temperature extremes, thermal cycling, impacts from micrometeoroids and orbital debris (MMOD), spacecraft self-contamination, and atomic oxygen (AO). While all of these environmental exposures can cause degradation to spacecraft components, AO is a particularly serious structural, thermal, and optical threat, especially to exterior oxidizable spacecraft components.

Atomic oxygen is formed in the LEO environment through photodissociation of diatomic oxygen (O_2). Short wavelength (<243 nm) solar radiation has sufficient energy to break the 5.12-eV O_2 diatomic bond in an environment where the mean free path is sufficiently long (~10^8 m) that the probability of re-association, or the formation of ozone (O_3), is small.[1,2] In LEO, between the altitudes of 180 and 650 km, AO is the most abundant species.[3]

A number of processes can take place when an oxygen atom strikes a spacecraft surface as a result of its orbital velocity and the thermal velocity of the atoms. These include chemical reaction with surface molecules, elastic scattering, scattering with partial or full thermal accommodation, and recombination or excitation of ram species, which consists predominantly of ground state $O(^3P)$ atomic oxygen atoms.[4] Atomic oxygen can react with polymers, carbon, and many metals to form oxygen bonds with atoms on the exposed surface. For most polymers, hydrogen abstraction, oxygen addition, or oxygen insertion can occur with the oxygen interaction pathways eventually leading to volatile oxidation products.[5,6] This results in gradual erosion of hydrocarbon or halocarbon material, with the exception of silicone materials. An example of the complete loss of a Kapton® H thermal blanket insulation layer, as well as degradation of other polymeric materials caused by AO erosion in LEO, is provided in Figure 1.[7] Even materials with AO protective coatings can be susceptible to AO erosion as a result of microscopic scratches, dust particles, or other imperfections in the substrate surface which can result in defects or pin windows in the protective coating.[8,9] These coating defects can provide pathways for AO attack, and undercutting erosion of the substrate can occur, even under directed ram AO exposure in LEO. One of the first examples of directed ram AO undercutting erosion in LEO was reported by de Groh and Banks for aluminized-Kapton insulation blankets from the Long Duration Exposure Facility (LDEF).[8]

The sensitivity of a hydrocarbon or halocarbon material to reaction with AO is quantified by the AO erosion yield, E_y, of the material. The AO E_y is the volume of a material that is removed (through oxidation) per incident oxygen atom and is measured in units of cm^3/atom. As AO erosion in LEO is a serious threat to spacecraft performance and durability, it is essential to know the LEO AO E_y so that the durability of materials being considered for spacecraft design can be predicted. The most well characterized AO E_y is that of polyimide Kapton H, which has an E_y of $3.0 \pm 0.07 \times 10^{-24}$ cm^3/atom for LEO 4.5-eV AO.[10-13]

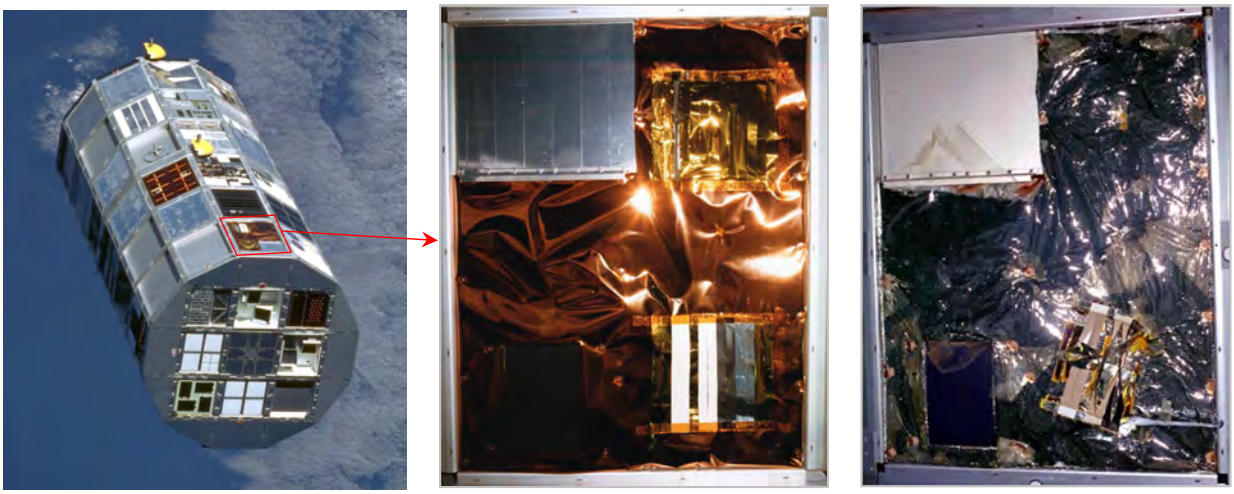

LDEF Tray F-9 pre-flight Tray F-9 post-flight

Figure 1. Atomic oxygen erosion of a Kapton® insulation blanket from Long Duration Exposure Facility (LDEF) experiment Tray F-9, located on the leading edge and exposed to direct-ram AO for 5.8 years.[7]

Another LEO threat to spacecraft materials is solar UV radiation, which has a typical wavelength of 0.1 to 0.4 micrometers.[14] Ultraviolet radiation is energetic enough to cause the breaking of organic bonds such as C=C, C=O, and C-H as well as other functional groups.[5] A molecule is raised to an excited state when an organic molecule absorbs a photon of UV radiation and bond dissociation can occur if the molecule acquires enough energy. Depending on the temperature and physical properties of the materials, the dissociated radical species are reactive intermediates, with the capability of diffusing several atomic distances from their point of origin and can participate in further reactions.[5] Solar radiation often results in bond breakage in materials as well as threats to functionality and stability of the materials. Therefore, solar radiation can possibly impact the erosion of some materials.

Because spaceflight materials exposure opportunities are rare, expensive, space-limited, and time-consuming, ground laboratory testing is often relied upon for spacecraft material environmental durability prediction. However, differences exist between ground facilities and actual space exposures, which may result in material-dependent differences in rates of reactions. Therefore, actual spaceflight AO E_y data are needed to best assess the durability of a material for spacecraft mission applicability. In addition, data from actual materials spaceflight experiments can be used to determine correlations between exposures in ground test facilities and space exposure, allowing for more accurate predictions of in-space materials performance based on ground facility testing. Materials spaceflight experiments for E_y determination have been flown on the Shuttle, the LDEF, the Russian space station Mir, and other spacecraft.[15] More recently, experiments have been flown as a part of the Materials International Space Station Experiment 1-8 (MISSE 1-8) missions flown on the exterior of the International Space Station (ISS).[9,15]

To further increase our understanding of the AO erosion of spacecraft materials, NASA Glenn Research Center developed and flew a passive experiment called the MISSE 7 Polymers Experiment. This is one of a series of NASA Glenn experiments flown as part of the MISSE missions for E_y determination.[9,16-20] The MISSE 7 Polymers Experiment was flown on the exterior of the ISS and exposed to the LEO space environment for 1.5 years. The primary objective of the MISSE 7 Polymers Experiment was to determine the LEO AO E_y of polymers and other materials. As part of the experiment a sample containing Class 2A diamond (100 plane) and highly oriented pyrolytic graphite (HOPG, basal and edge planes) was exposed to ram AO and characterized for erosion. This paper provides an overview of the MISSE 7 mission, a description of the MISSE 7 Polymers Experiment, pre-flight and post-flight characterization techniques, the AO fluence for the LEO ram exposure, and the AO E_y results for diamond and HOPG. The data is compared to prior shuttle flight E_y values for diamond and the E_y of pyrolytic graphite exposed to four years of space exposure as part of the MISSE 2 mission. The E_y data from this ISS spaceflight experiment provides valuable information for LEO spacecraft design.

Materials International Space Station Experiment (MISSE) Overview

The MISSE program involves is a series of spaceflight missions with experiments flown on the exterior of the ISS to test the performance and durability of materials and devices exposed to the LEO space environment. In the MISSE 1-8 missions, individual flight experiments were flown in suitcase-like containers called Passive Experiment Containers (PECs) that provide exposure to the space environment. The PECs were closed during launch to protect the samples. Once on orbit, the PECs were placed on the exterior of the ISS during an extravehicular activity (EVA), or spacewalk, in either a ram/wake or a zenith/nadir orientation and opened exposing the experiments to the space environment for the duration of the mission. A diagram showing ram, wake, zenith, and nadir directions on the ISS is shown in Figure 2. The flight orientation highly affects the environmental exposure. Ram facing experiments receive a high flux of directed AO and sweeping (moderate) solar exposure. Zenith facing experiments receive a low flux of grazing arrival AO and the highest solar exposure. Wake experiments receive very low AO flux and moderate solar radiation (levels similar to ram experiments). Nadir experiments receive a low flux of grazing arrival AO and minimal solar radiation (albedo sunlight). All surfaces receive charged particle and cosmic radiation, which are omni-directional. It should be noted that the actual orientation of the ISS varies due to operational requirements with the majority of the time spent within ±15 degrees of the +XVV Z nadir flight attitude (X Axis Near Velocity Vector, Z Axis Nadir/Down). Deviations from this attitude to accommodate visiting spacecraft, and other ISS operational needs, can cause variations in the orientation directions, and hence variations in environmental exposures especially for atomic oxygen exposure of zenith and nadir surfaces.

The MISSE 7 mission consisted of two PECs called MISSE 7A and 7B, which were flown in zenith/nadir and ram/wake orientations, respectively, on the ISS EXPRESS Logistic Carrier 2 (ELC-2) site. MISSE 7A and 7B were placed on the exterior of the ISS during the STS-129 Shuttle mission on November 23, 2009 and retrieved during the STS-134 Shuttle mission on May 20, 2011 after 1.49 years of space exposure. Figure 3 shows the location of MISSEs 7A & 7B on the ISS ELC-2. Figure 4 shows the zenith side of MISSE 7A and the ram side of 7B as imaged during the STS-130 mission in February 2010.

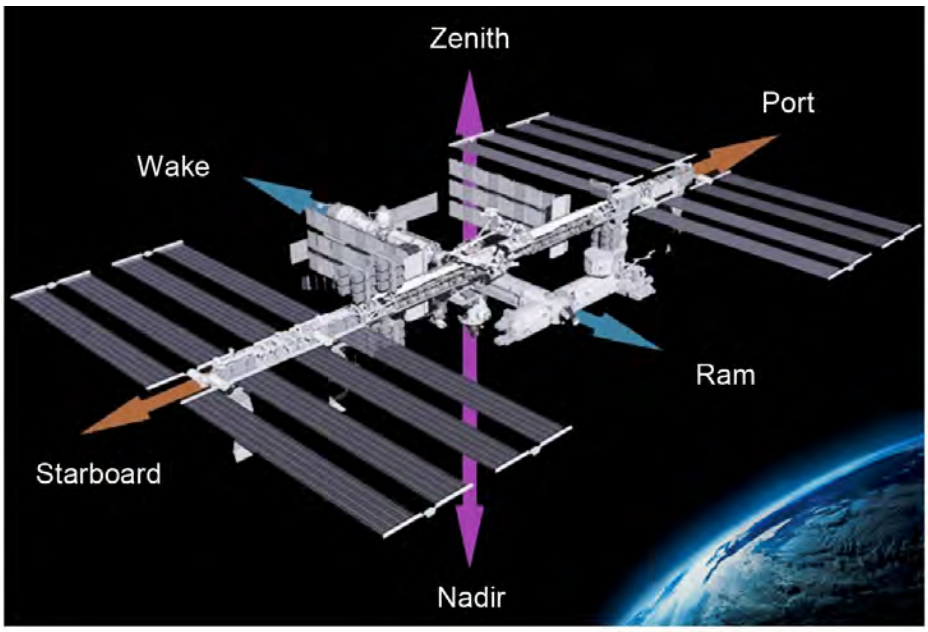

Figure 2. Diagram showing ram (flight direction), wake, zenith, and nadir directions on the International Space Station.

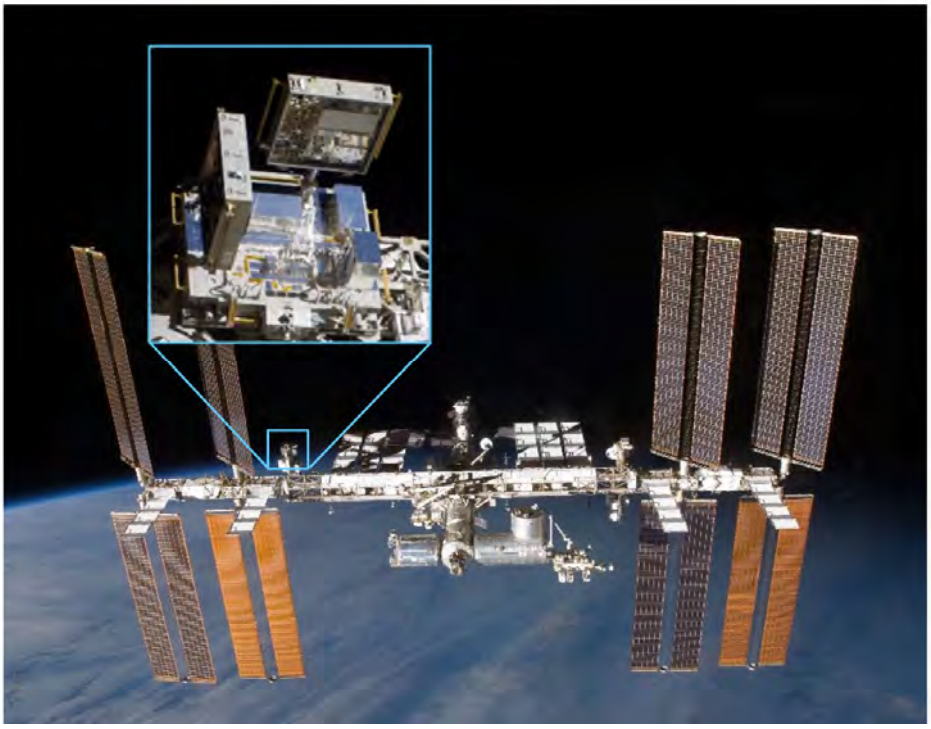

Figure 3. Location of MISSEs 7A & 7B on the ISS ELC-2 as imaged during the STS-129 shuttle mission in November 2009 shortly after deployment.

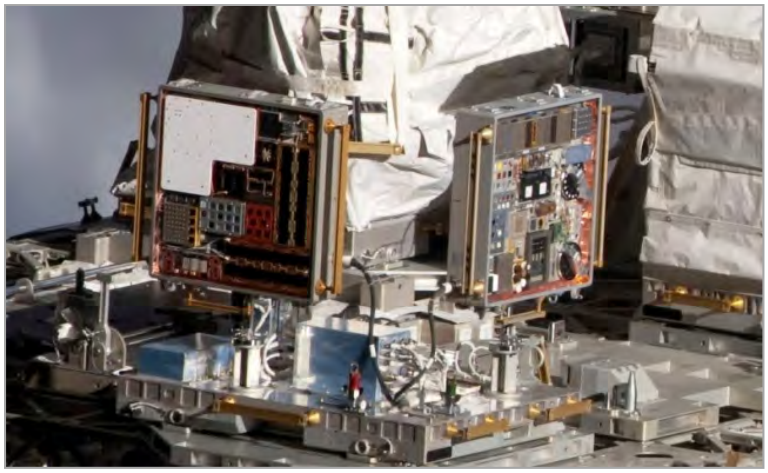

Figure 4. On-orbit photo of MISSE 7A (left, zenith surface shown) and 7B (right, ram surface shown) as imaged during the STS-130 shuttle mission in February 2010.

MISSE 7B Polymers Experiment

The MISSE 7B Polymers Experiment was a passive experiment with 45 samples, which were flown in ram and wake orientations on MISSE 7B. The primary objective of the Polymers Experiment was to determine the LEO AO E_y of various polymers and other materials. Tensile samples were also included to assess space induced mechanical property degradation of Teflon. Thirty-eight samples were flown in the ram direction, exposing them to high AO and solar radiation. Thirty of the ram samples were flown for E_y evaluation (27 for mass-based E_y determination and 3 for recession depth based E_y determination). Six ram tensile samples were flown for mechanical property assessment. A Kapton H sample (B7-8) was flown for AO fluence determination and a fused alumina (Al_2O_3) sample was flown for contamination analyses. Seven samples (5 E_y and 2 tensile) were flown in the wake orientation, exposing them to solar radiation with minimal AO. Additional MISSE 7 Polymer Experiment details are provided in references 18, 19 and 21 with previously reported mass based E_y values provided in references 18 and 19 and tensile data provided in reference 21.

MISSE 7B Sample B7-6

As part of the MISSE 7B Polymers Experiment, sample B7-6, containing diamond and highly oriented pyrolytic graphite (HOPG) was exposed to ram AO and characterized for E_y based on recession depth measurements. Sample B7-6 was flown in Tray B7-R which held 1" (2.54 cm) square samples. A pre-flight photo of the Tray B7-R is shown in Figure 5, and the location of B7-6 is indicated on the image.

Sample B7-6 consisted of three types of materials: 1). three small Class 2A diamond (100 plane) squares, 2). A piece of HOPG mounted with the basal plane facing the ram direction, and 3). Four pieces of HOPG mounted with the edge plane (perpendicular to the basal plane) facing the ram direction. All materials were adhered to an Al substrate using epoxy resin. A preflight photo of the B7-6 sample mounted in the B7-R Tray is provided in Figure 6. The sample was salt-sprayed prior to flight to provide isolated AO protection on each material for post-flight recession depth measurements.

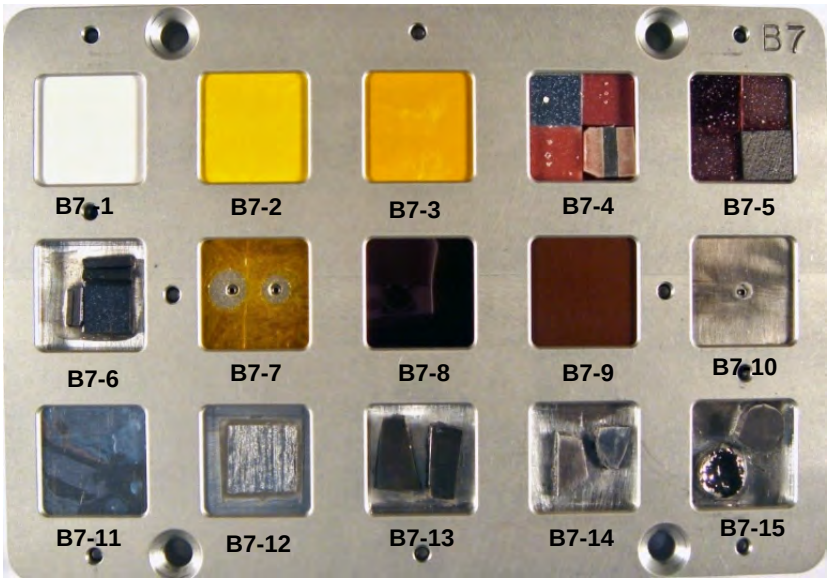

Figure 5. Pre-flight photo of the MISSE 7 B7-R tray with sample IDs. B7-6 is the sample with Diamond and HOPG. Samples B7-12 to B-15 are not part of the Polymers Experiment.

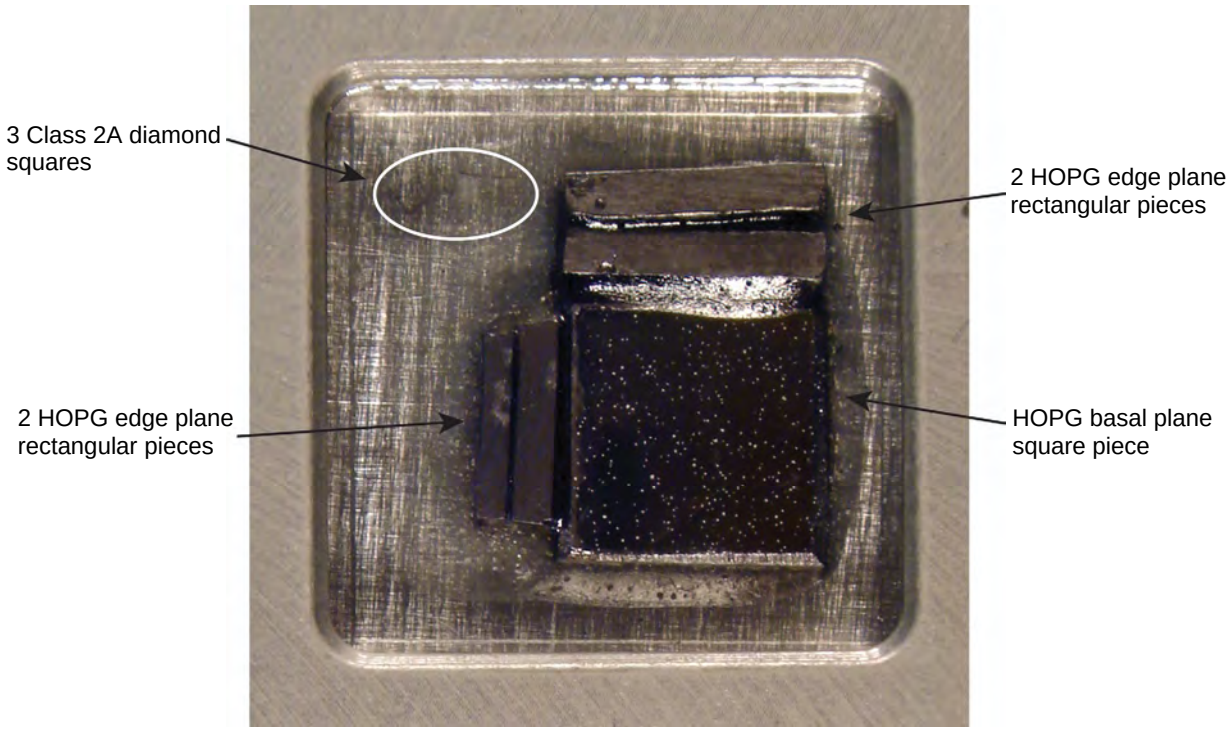

Figure 6. Pre-flight photo of the B7-6 sample mounted in the MISSE 7 B7-R tray.

Experimental Procedures

Recession Depth Based Erosion Yield

Recession measurements can be used for AO E_y determination based on erosion depth step-heights. The erosion or recession depth (D) can be measured from a protected surface using profilometry, scanning electron microscopy (SEM), optical interferometry or atomic force microscopy for low fluence exposures.[22] The erosion yield, E_y, can be calculated through the following equation:

$$E_y = D/F \tag{1}$$

Where

E_y= *erosion yield of flight sample (cm^3/atom)*
D= *erosion depth of flight sample (cm)*
F= *low Earth orbit AO fluence (atoms/cm^2)*

The recession depth technique used for this flight sample involves pre-flight protection of the sample surface using isolated small salt (NaCl) particles that are in intimate contact with the sample.[22,23] The salt particles are applied to the sample substrate by spraying a saturated salt solution using an atomizer. This results in isolated protective particles that typically remain in contact on the surface during flight and retrieval. The particles are then removed post-flight by washing off the salt with distilled water followed by drying with nitrogen gas.[22,23] The recession depth was then determined using scanning electron microscopy, as indicated below.

Field Emission Scanning Electron Microscopy

The erosion depth was determined using a Hitachi S-4700 field emission scanning electron microscope (FESEM) operated at an accelerating voltage of 6 kV. The sample was coated with 7.5 nm of Pt prior to imaging in the FESEM. Images were obtained at 0 and 40 degree tilt angles, and the recession depth (D) was determined using the equation:

$$D = d/\mathrm{Sin}\ \theta \tag{2}$$

Where

D= *erosion depth of flight sample (cm)*
d= *erosion depth measured from SEM image obtained at θ tile angle (cm)*
θ= *SEM tilt angle (degrees)*

The SEM image based erosion depth (d) was measured from the top of the protected surface to the mid-length of the left standing erosion cones. Energy dispersive spectroscopy (EDS) analysis was conducted using an Oxford Instruments X-Max Detector and AZtek software system to look for evidence of contamination, which would affect erosion.

Atomic Oxygen Fluence Determination

Atomic oxygen fluence (*F*) was determined through the mass loss of a Kapton H witness sample (B7-8) because Kapton H has a well characterized erosion yield, E_K (3.0×10^{-24} cm^3/atom) in the LEO environment.[10-13] The AO fluence can be calculated using the following equation:

$$F = \frac{\Delta M_K}{\left(A_K \rho_K E_K\right)} \tag{3}$$

Where

F= *low Earth orbit AO fluence (atoms/cm^2)*
ΔM_K = *mass loss of Kapton H witness sample (g)*
A_K = *surface area of Kapton H witness sample exposed to AO (cm^2)*
ρ_K = *density of Kapton H witness sample (1.4273 g/cm^3)*[2]
E_K = *erosion yield of Kapton H witness sample (3.0×10^{-24} cm^3/atom)*

Photo Documentation

Sony DSC-T7 and Fujifilm FinePix S1500 digital cameras were used to take pre and/or post-flight macro photos of the flight sample. An Olympus SZH optical microscope (OM) operated with a Leica DFC29S camera was used to take post-flight images of the sample at higher magnification.

Results and Discussion

Atomic Oxygen Fluence and Solar Exposure

The mass loss, surface area, density, E_y and computed fluence for the ram Kapton H fluence sample (B7-8) is provided in Table 1. The AO fluence for the MISSE 7B ram tray was determined to be 4.22×10^{21} atoms/cm^2.[18,19] Similar ram fluence values ($4.2 \pm 0.1 \times 10^{21}$ atoms/cm^2) have been reported by Finckenor based on mass loss and thickness loss of Kapton HN, using an E_y of 2.81×10^{-24}.[2,16,24]

Table 1. Atomic Oxygen Fluence for the MISSE 7 Ram samples.

MISSE 7 Tray	Sample ID	Material	Mass Loss (g)	Surface Area (cm^2)	Density (g/cm^3)	Kapton E_y (cm^3/atom)	MISSE 7 Fluence (atom/cm^2)
B7-R	B7-8	Kapton H	0.077547	4.291	1.4273	3.00E-24	4.22E+21

Estimates of solar exposure in equivalent sun hours (ESH) have been determined for the MISSE 7 ram surfaces. The ram surface received an estimated 2,400 ESH based on UV diode measurements on readings from ram and wake trays, respectively, monitored by the Lead-Free Technology Experiment in Space Environment.[25]

Post-flight Observations

Upon initial post-flight inspection the B7-6 sample showed discoloration of the epoxy resin. This can be seen by comparing the post-flight photo of the B7-R tray, shown in Figure 7 with the pre-flight photo provided in Figure 5. The discolored epoxy resin can also be seen in the post-flight photograph of the B7-6 sample shown in Figure 8. Fortunately, the majority of the salt particles remained intact after flight. The particles can be seen in the enlarged image of a section of the basal plane HOPG shown in Figure 8. Figure 9 provides post-flight photographs of the sample before, and after, the salt was rinsed off with a distilled water rinse. The post-rinse image shows that the salt particles were successfully removed during the rinse procedure. This can be seen in Figure 9b as dark spots are left where the "white" salt particles protected the sample from erosion.

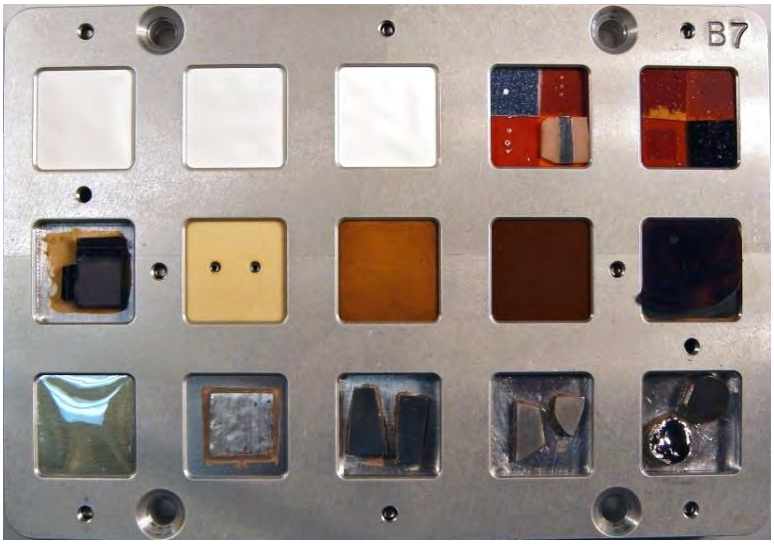

Figure 7. Post-flight photograph of the MISSE 7 B7-R tray.

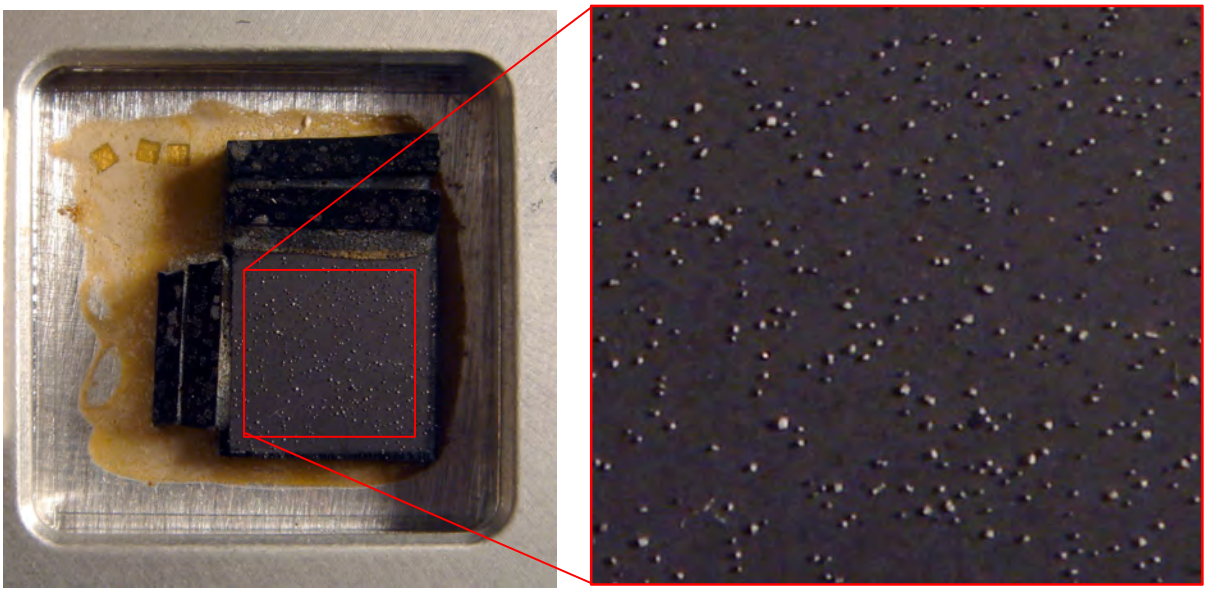

Figure 8. Post-flight photograph of the sample B7-6 in the B7-R tray, with a close-up image showing the salt-particles on the basal plane HOPG.

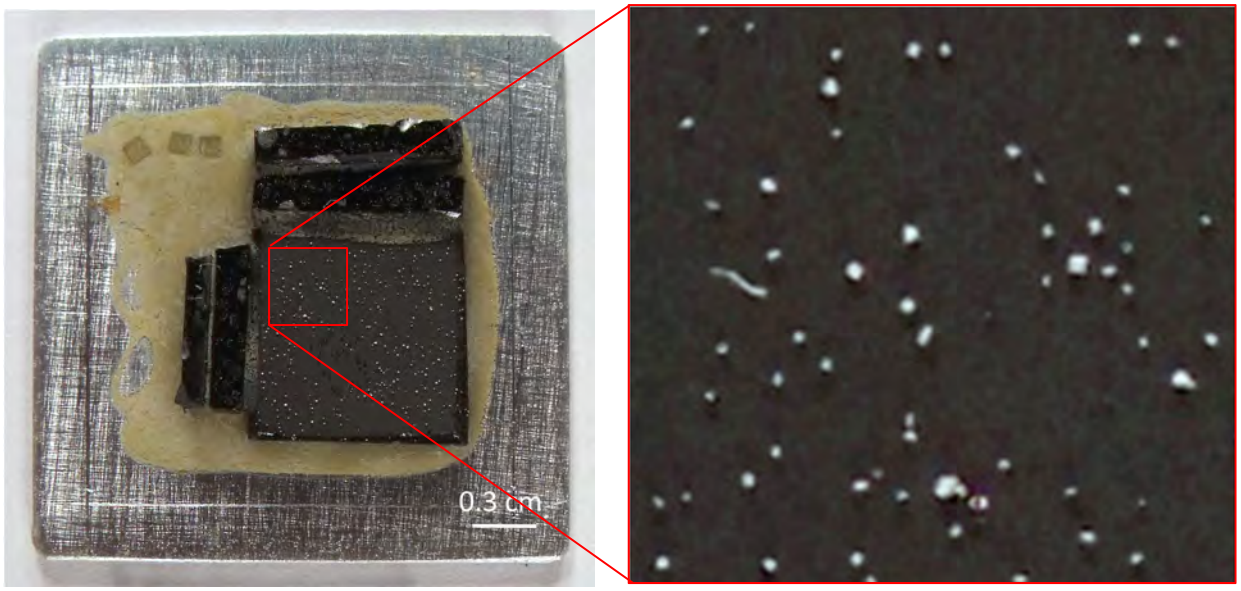

a.

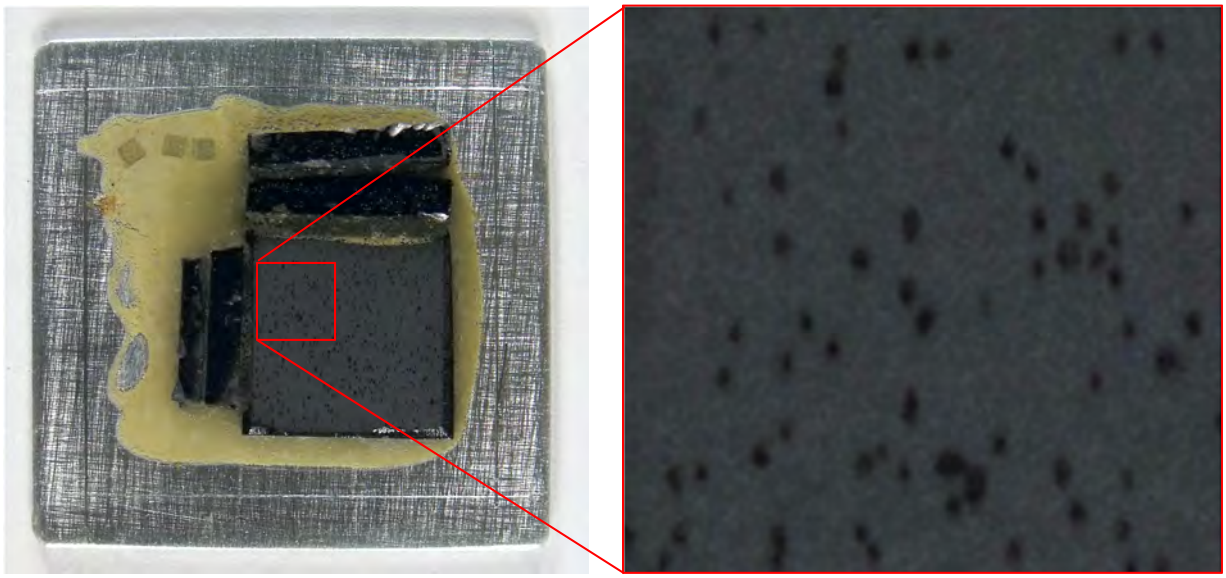

b.

Figure 9. Post-flight photographs of the sample B7-6: a). Prior to salt removal showing bright salt particles, and b). After salt removal showing dark areas that were protected from AO erosion.

Erosion Yield Results

Diamond

Figure 10 is an optical microscope image of the three diamond particles after the salt was removed. Figure 11 shows one of the diamond particles prior to salt removal (Figure 11a) and after salt removal (Figure 11b). Figure 12a is a scanning electron microscope (SEM) image of two diamond particles after the salt has been removed. Figure 12b is a SEM image that shows a large salt protected area. In this image the smooth, non-eroded, salt protected surface appears darker than the AO exposed and eroded neighboring surface. Figure 13a provides a close-up image of a protected-AO exposed border of the salt protected area shown in Figure 12b. Figure 13b is a 10,000 X magnification image of the salt protected area, showing a very smooth non-eroded surface texture. Figure 13c is a 10,000 X imagination image of an AO exposed area showing erosion texture. Evidence of erosion texture was a surprising result as a single crystal Class IIA diamond sample flown on the Evaluation of Oxygen Interactions with Materials III (EOIM-III) shuttle flight experiment appeared to have no notable erosion with a measured E_y of $0.0000 \pm 0.000023 \times 10^{-24}$ cm^3/atom based on stylus profilometry.[26] It should be noted that the AO fluence for the shuttle flight experiment was 2.3×10^{20} atoms/cm^3, which is 18X less than the fluence for the MISSE 7 ram exposure.

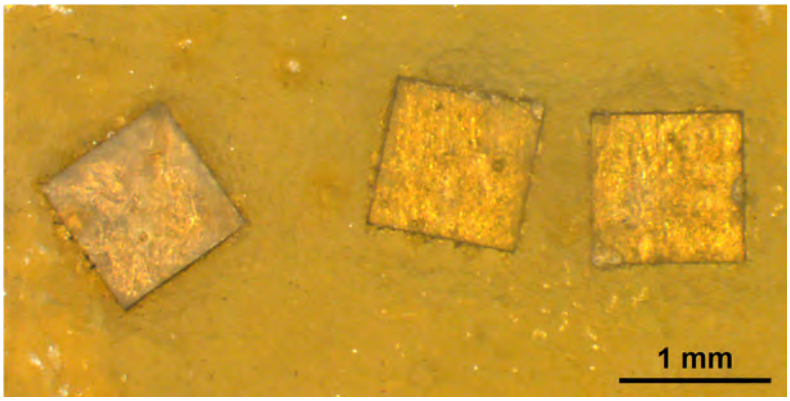

Figure 10. Post-flight optical micrograph of the three diamond particles with the salt removed.

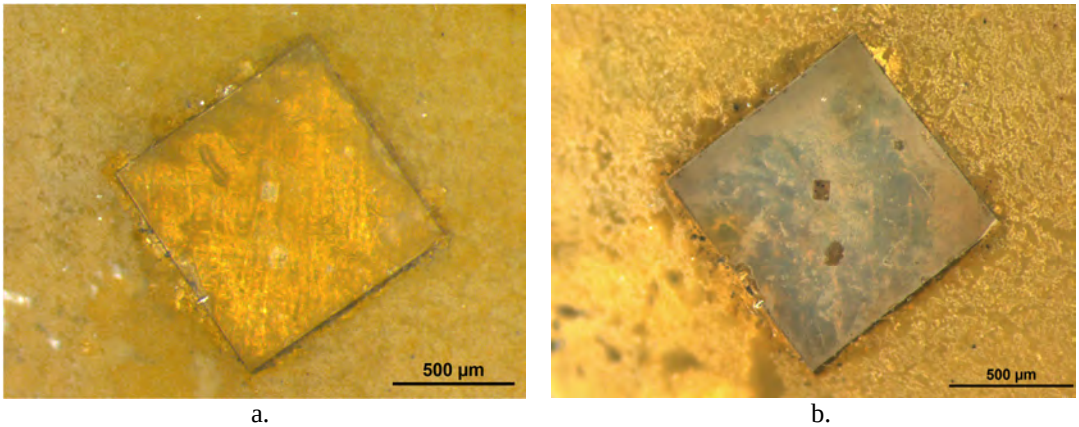

a. b.

Figure 11. Optical microscope images of diamond Particle 1: a). Prior to salt removal, and b). After salt removal where the dark area is the AO protected surface.

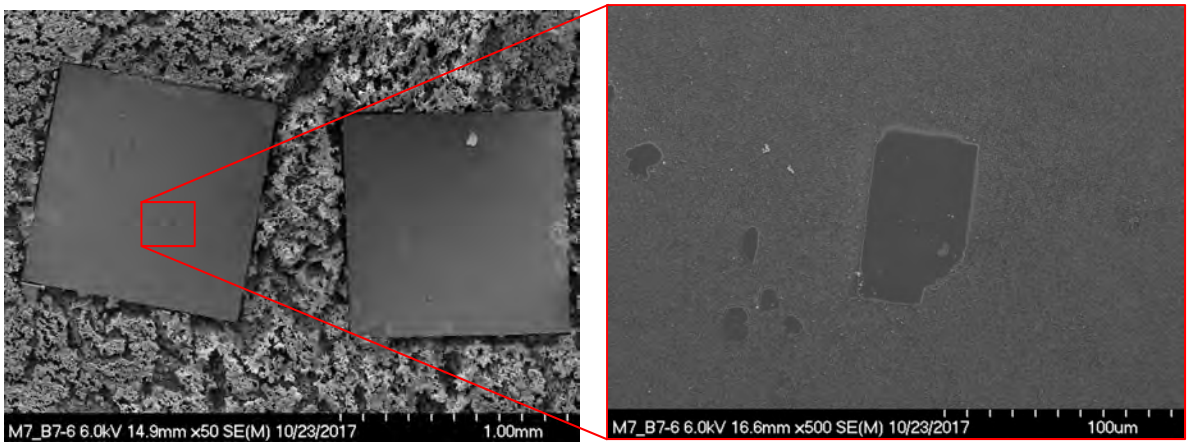

a. b.

Figure 12. SEM images (0° tilt) of diamond particles: a). Low magnification image showing diamond particle #2 (left) and diamond particle #3 (right), and b). A large salt-protected area on diamond particle #2.

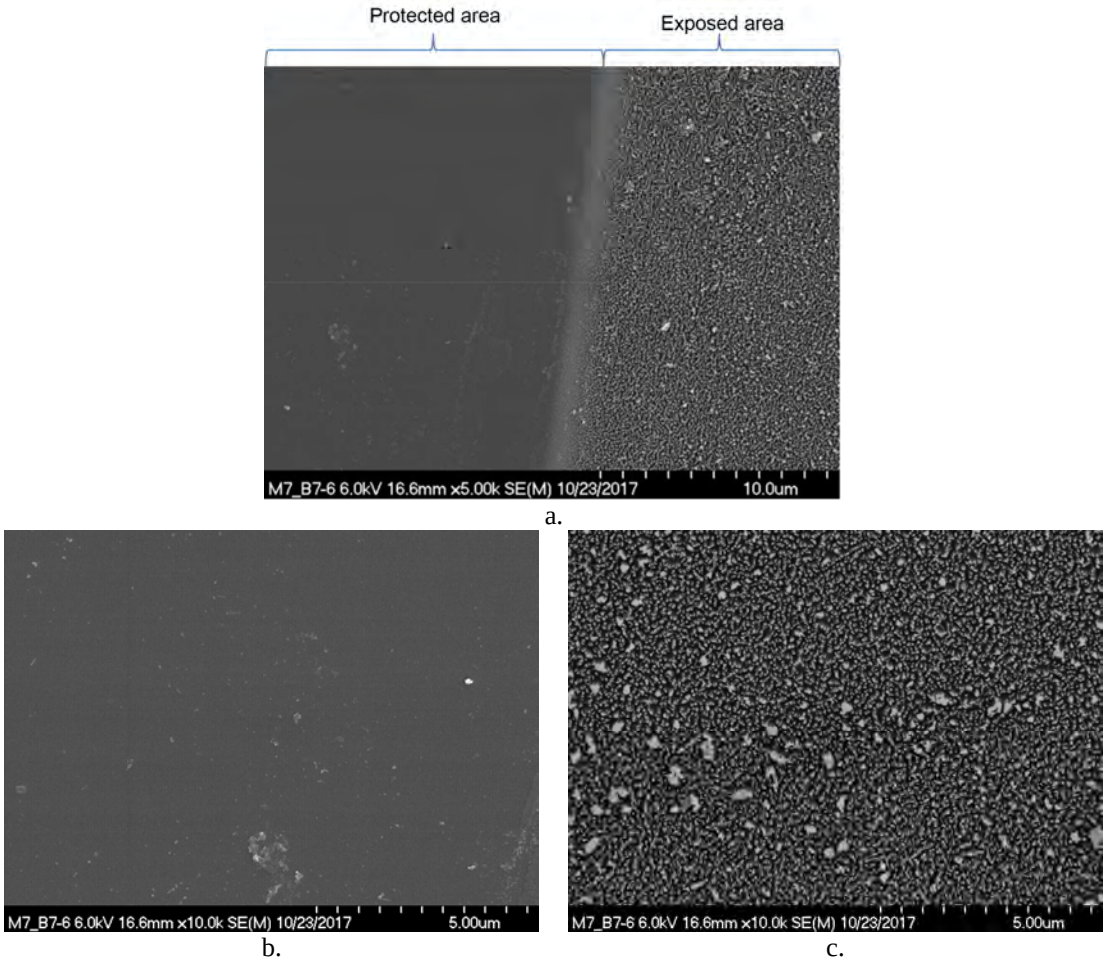

a.

b. c.

Figure 13. SEM images (0° tilt) of diamond particle #2: a). Image showing protected (left) and AO exposed (right) regions, b). Image of a salt-protected area showing the smooth, non-eroded surface texture, and c). Image of an exposed area showing AO erosion texture.

The image areas shown in Figure 13b (protected) and 13c (AO eroded) were analyzed using EDS to look for any contamination, such as silicone contamination which can affect AO erosion. Both of the areas analyzed displayed only C and Pt peaks, see Figure 14. When the EDS software accounted for the 7.5 nm Pt coating, both areas analyzed had 100 weight percent C. Hence, no contamination was detected.

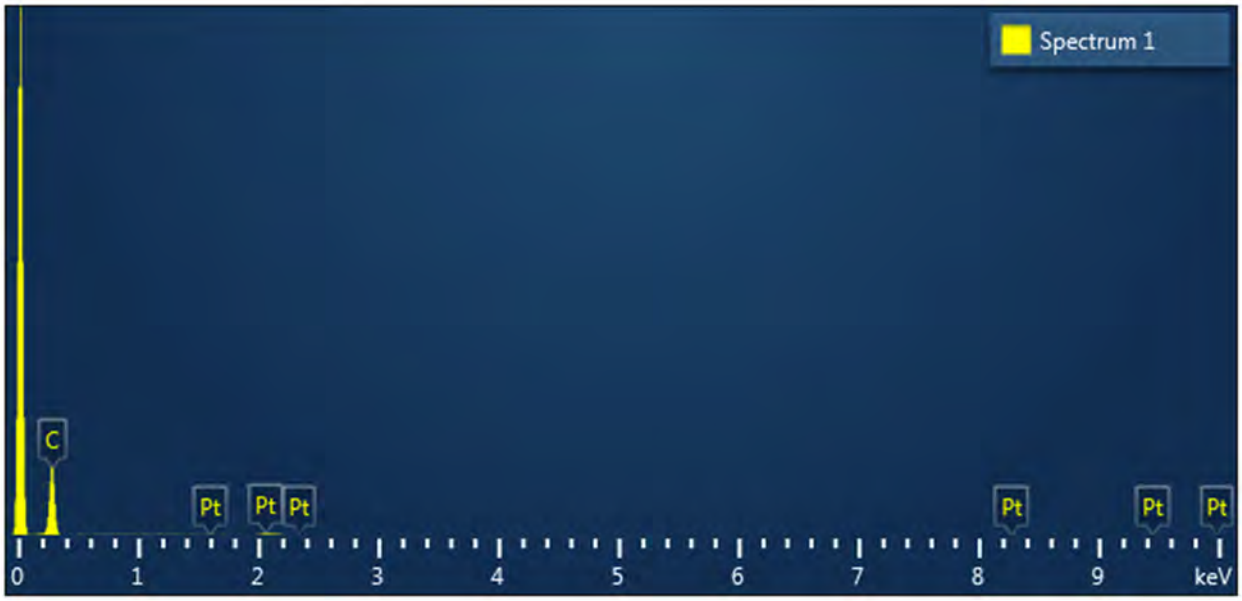

a.

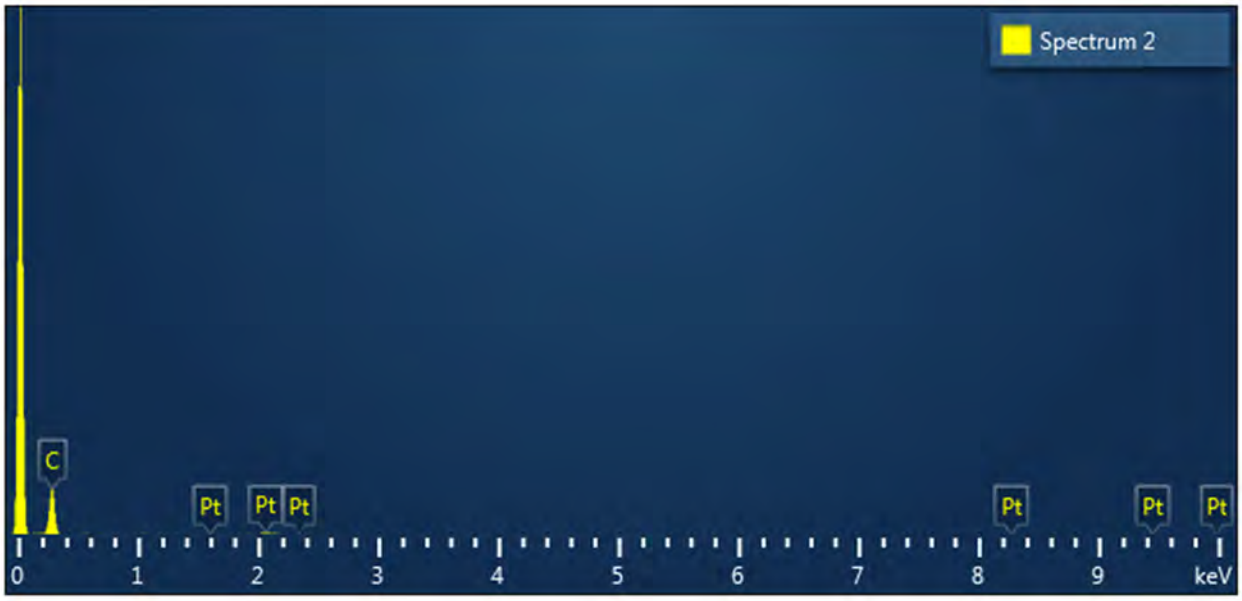

b.

Figure 14. Energy dispersive spectroscopy spectra: a). Protected area that was under the salt particle shown in Figure 13b, and b). Unprotected area shown in Figure 13c.

Scanning electron microscope images of the AO eroded texture of the Class 2A diamond taken at 40° tilt angles are provided in Figure 15. Figure 15a is a 10kX magnification image showing the AO eroded texture. Figure 15b is a 40kX magnification image of the AO eroded texture showing the typical AO erosion cones that develop with directed ram AO exposure. Figure 15c is a 25kX magnification image of a salt protected (top) and AO exposed (bottom) border. The erosion depth (d) measurements were obtained from the SEM image provided in Figure 15c. The E_y was based on six different erosion depth (d) measurements measured from the SEM image and was determined to be $1.58 \pm 0.40 \times 10^{-26}$ cm^3/atom. Therefore, Class 2A diamond (100 plane) does erode with AO exposure, but it has an extremely low E_y (300X less than Kapton H). The ratio of texture height (A) to the actual erosion depth (D), A/D, was also measured and determined to be 0.879 based on eight different measurements. Thus, because the tops of the cones are so close to the un-eroded surface of the diamond, it is believed that the stylus profilometry used to measure the E_y for the Class IIA diamond flown on EOIM-III may have simply glided over the tops of the small erosion cones, and the vast majority of the erosion occurred in the space between the small cones which was not measured.

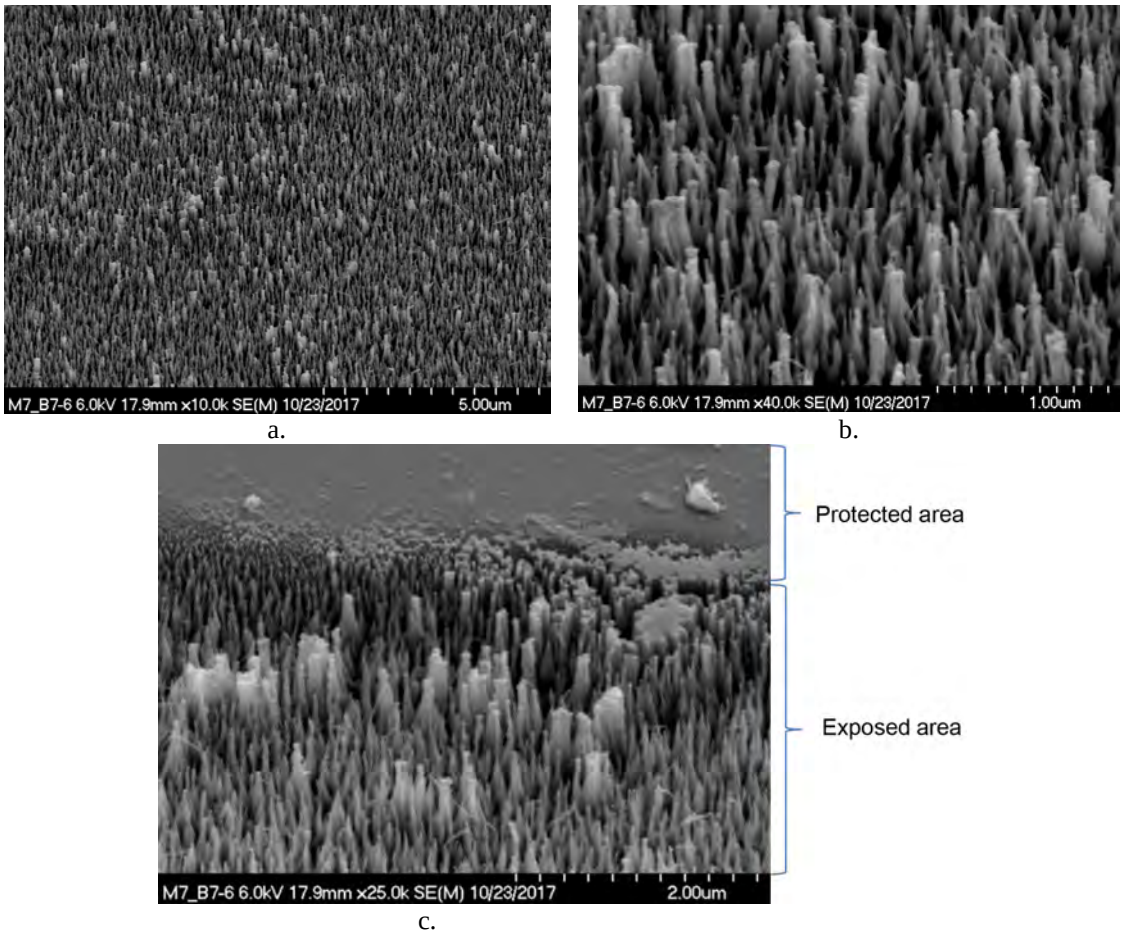

Figure 15. SEM images (40° tilt) of diamond particle #2: a). Image showing AO eroded texture, b). Image of the AO eroded texture at a higher magnification, and c). Image of a protected (top) and AO exposed (bottom) border.

Basal Plane HOPG

Figure 16 provides optical microscope images of the basal plane HOPG sample prior to salt removal (Figure 16a) and after salt removal (Figure 16b). In Figure 16a, the salt particles appear bright, but there is a region of dark spots which is where the salt has fallen off likely due to post-flight handling. In Figure 16b those areas protected by the salt particles appear dark after the salt has been removed. Figure 17 provides higher magnification optical microscope images of the basal plane HOPG. Figure 17a is an image prior to salt removal with bright salt particles. Figure 17b is an image after salt removal where the dark areas are the AO protected areas. Figure 17c is a close-up image of salt-protected areas or "buttes".

Figure 18 provides SEM images taken at a 0° tilt of the basal plane HOPG sample. Figure 18a is a low magnification image (50X) showing a number of salt protected areas. Figure 18b shows a group of seven salt-protected buttes. Figure 19 is an SEM image taken at a 0° tilt angle of a basal plane HOPG protected butte with close-up images of the edge texture.

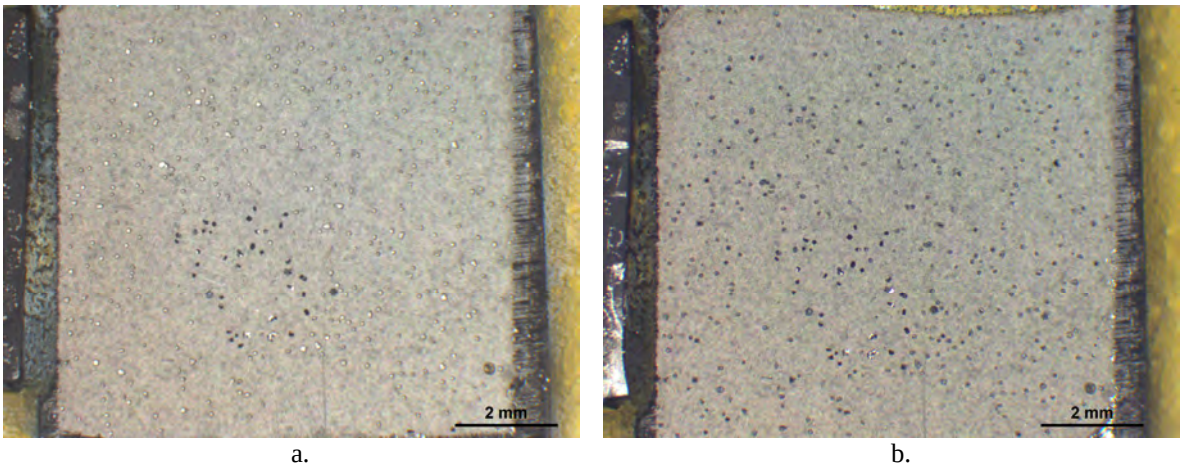

a. b.

Figure 16. Optical microscope mages of the basal plane HOPG: a). Prior to salt removal, and b). After salt removal where the dark areas are the AO protected regions.

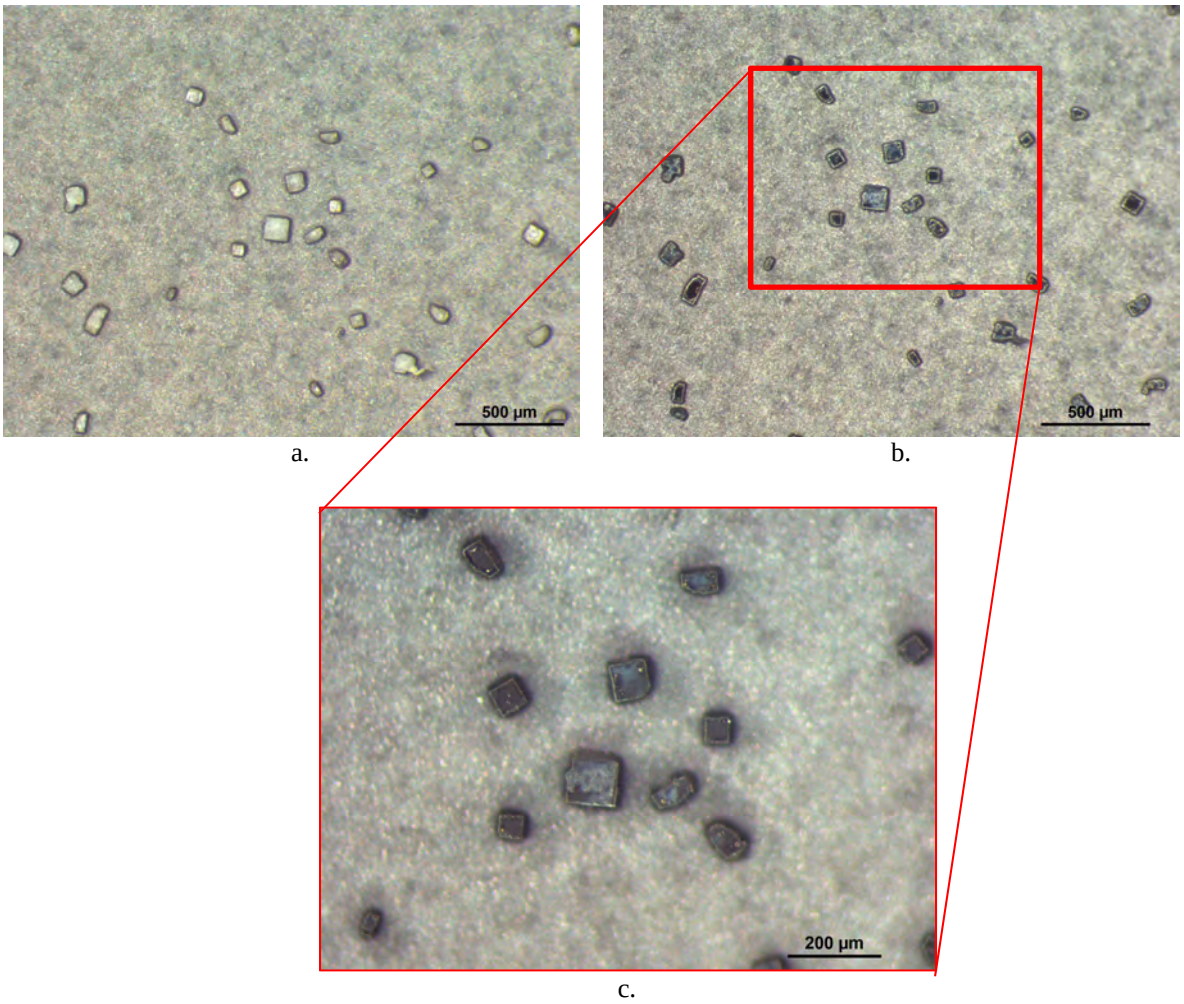

a. b. c.

Figure 17. Higher magnification optical microscope images of the basal plane HOPG: a). Prior to salt removal with bright salt particles, b). After salt removal where the dark areas are the AO protected regions, and c). Close-up image of salt-protected areas.

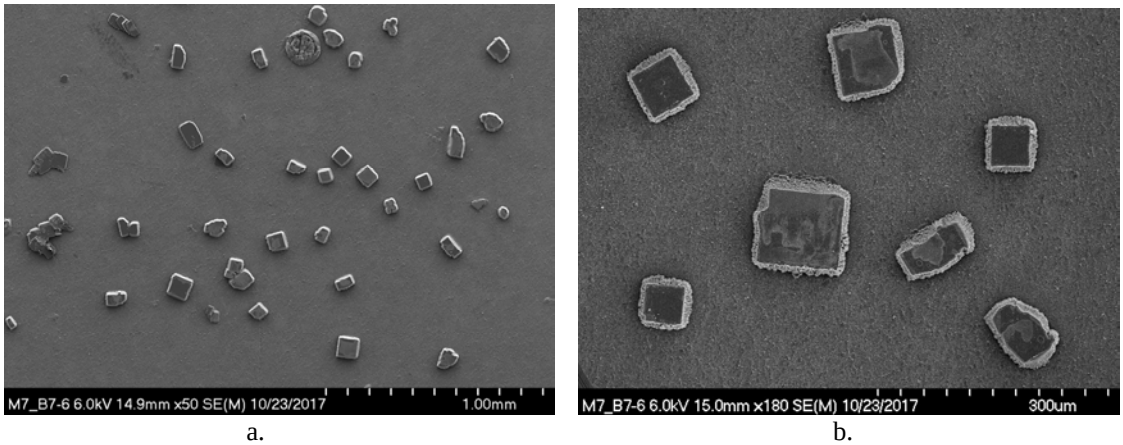

a. b.

Figure 18. Electron microscope images (0° tilt) of the basal plane HOPG sample: a). 50X magnification showing a number of salt protected areas, and b). 180X magnification showing a group of seven salt-protected buttes (the same buttes seen in Figure 17c).

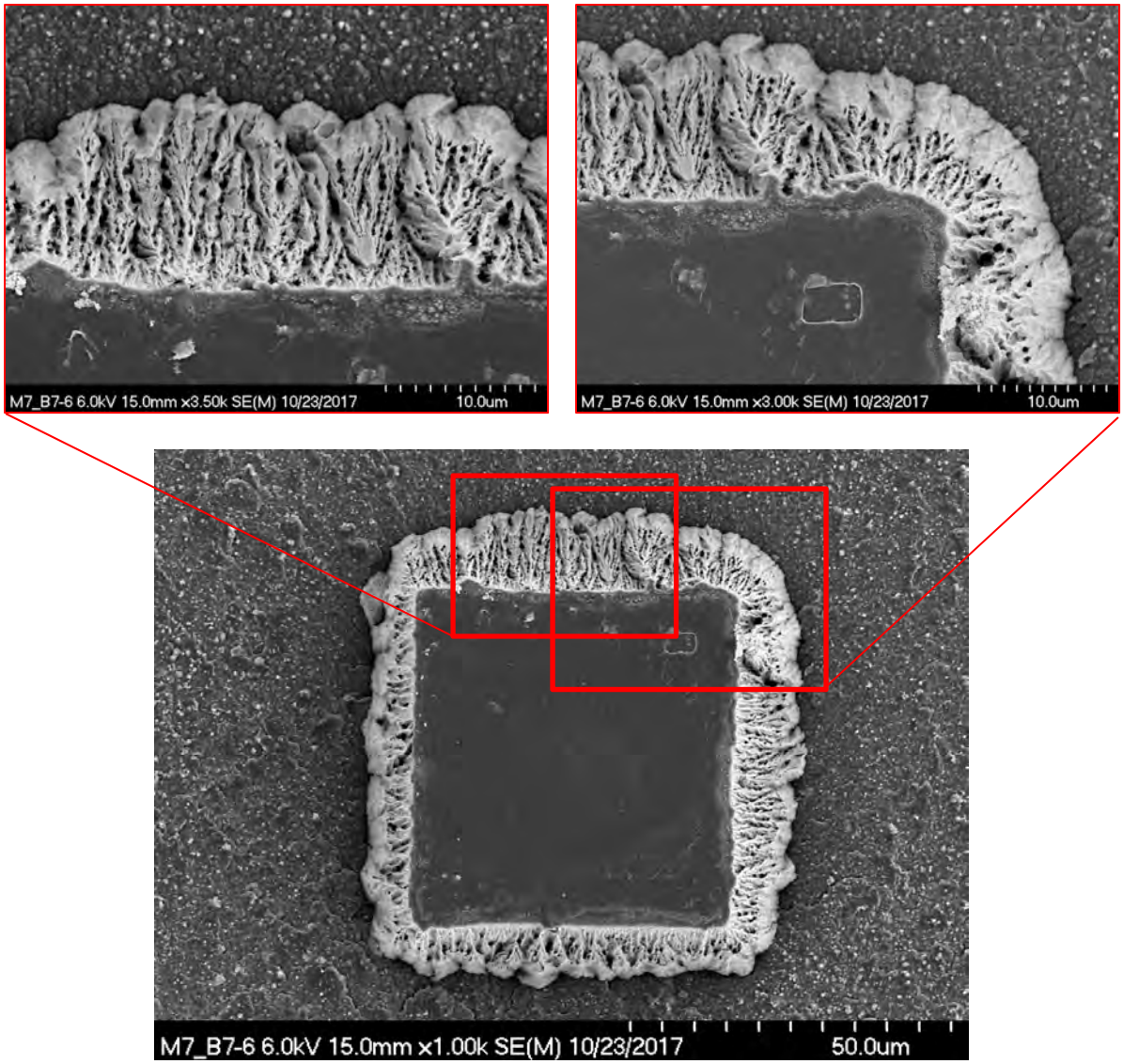

Figure 19. Electron microscope image (0° tilt) of a basal plane HOPG protected butte with close-up images of the edge texture.

Figure 20 provides electron microscope images taken at a 40° tilt angle showing the group of seven salt-protected buttes shown in 18b. This image shows that the salt particles successfully protected the underlying area from AO erosion. Thus, AO protected "buttes" remain. This image also shows that the basal plane HOPG was significantly more eroded than the diamond. Figure 21 shows two protected buttes along with close-up images. The erosion depth (d) measurements were obtained from SEM images such as those provided in Figure 21b and 21d. The furrowed nature of the slope between the protected area and the eroded area may be caused by the microscopically irregular edge of the protected area and the scattering of AO by the edge of the salt particle. The E_y of the basal plane HOPG was based on eight different measurements and was determined to be $1.05 \pm 0.08 \times 10^{-24}$ cm^3/atom.

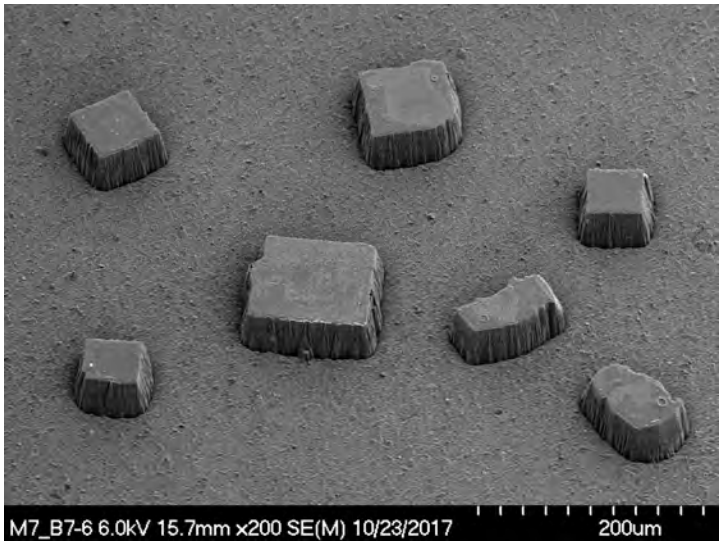

Figure 20. Electron microscope image (40° tilt) of the basal plane HOPG sample showing a group of seven salt-protected buttes.

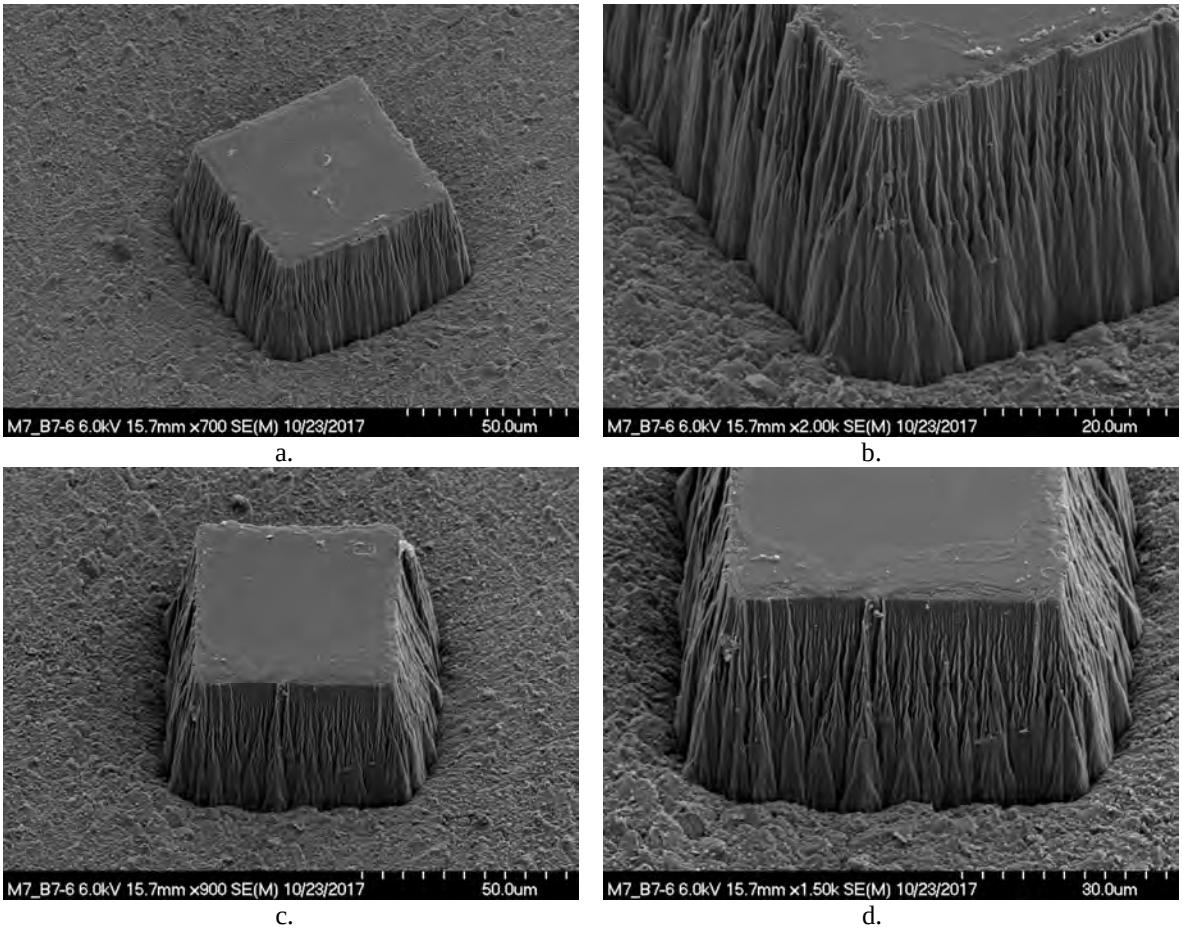

a. b.

c. d.

Figure 21. SEM images (40° tilt) of protected buttes on the basal plane HOPG sample: a). A salt protected butte, b). Close-up of the butte shown in 21a, c). A second salt protected butte, and d). Close-up of the butte shown in 21c.

Figures 22a-f and Figure 23 shows the erosion texture of the HOPG basal plane. This texture is not typical of AO erosion of organic materials with volatile oxides. Typically, with direct ram exposure, such as the MISSE 7 ram samples experience, cone-like textures develop such as the diamond erosion "cones" shown in Figure 15b. The texture height (A) to actual erosion depth (D) ratio was computed for the basal plane HOPG based on 8 different measurements and was determined to be 0.016. This is significantly lower than for most polymers and probably indicates that scattering of AO off the edges of HOPG planes causes erosion of any cones that start to form, which results in a reasonably smooth texture. Such phenomena would enable isotropic graphite to develop significant cones because of the random orientation of the graphitic structure.

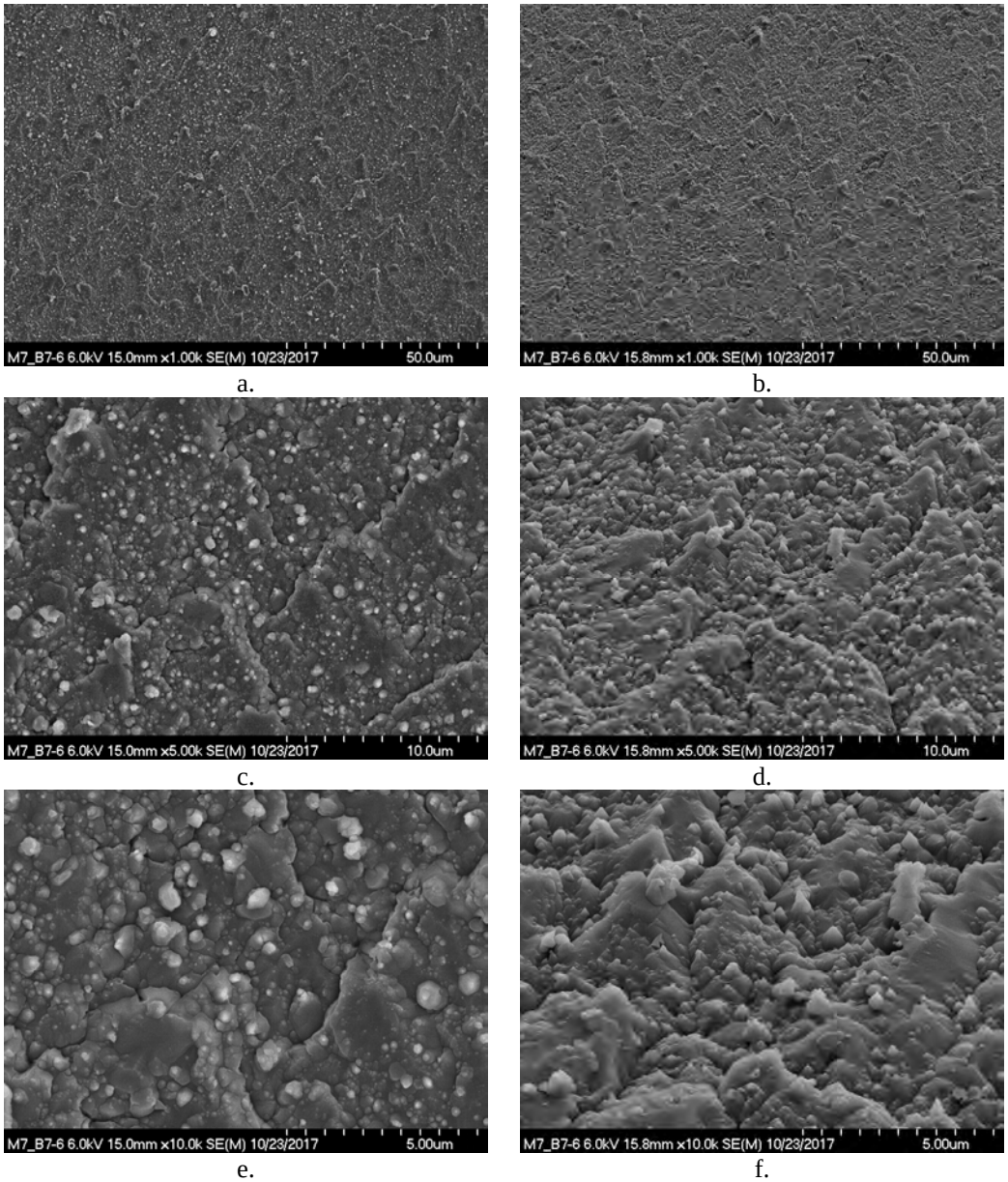

Figure 22. SEM images (0° tilt and 40° tilt) of the AO erosion texture of the basal plane HOPG: a). 1kX magnification at 0° tilt, b). 1kX magnification at 40° tilt (same area as 22a), c). 5kX magnification at 0° tilt, d). 5kX magnification at 40° tilt (same area as 22c), e). 10kX magnification at 0° tilt, f). 10kX magnification at 40° tilt (same area as 22e).

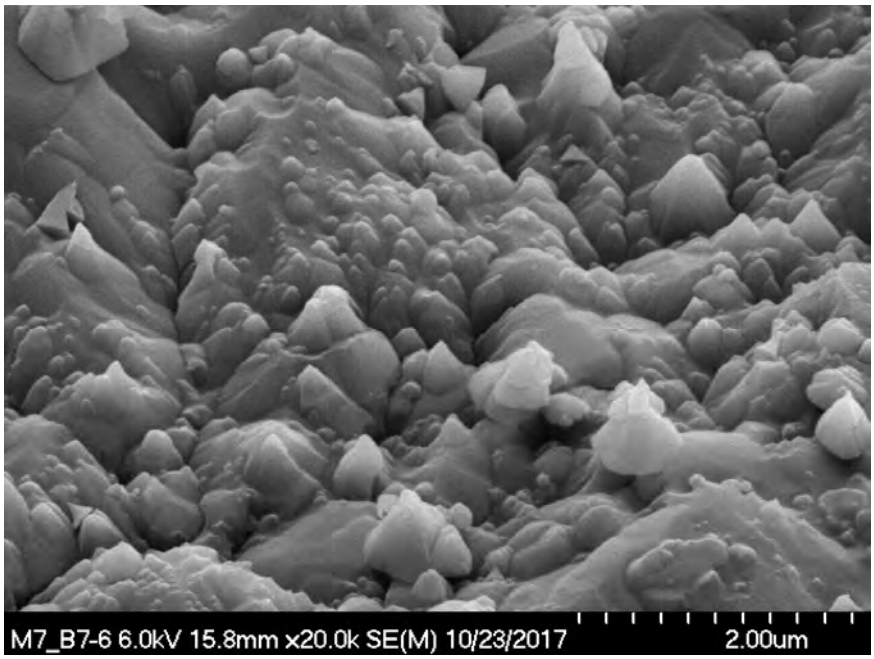

Figure 23. SEM image at 40° tilt showing the AO erosion texture of the basal plane HOPG.

Edge Plane HOPG

Figure 24 provides optical microscope images of the edge plane HOPG sample prior to salt removal (Figure 24a) and after salt removal (Figure 24b). The image after salt removal looks very similar to the image with the salt, but the salt protected areas appear very bright after removal as those areas are smooth and reflect the microscope light. Figure 25 provides an optical microscope image with a corresponding electron microscope image in the same area showing salt protected areas.

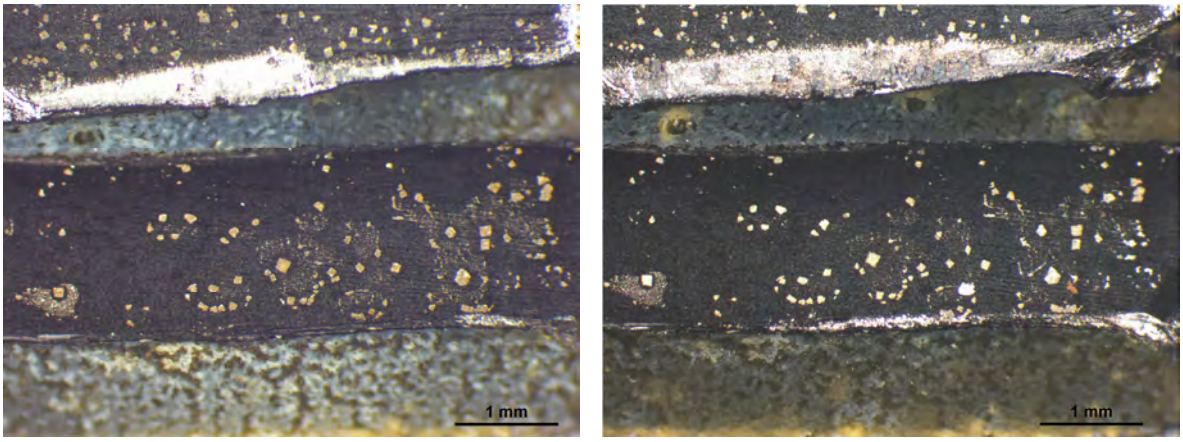

a. b.

Figure 24. Optical microscope mages of the edge plane HOPG: a). Prior to salt removal, and b). After salt removal where the salt protected areas appear bright.

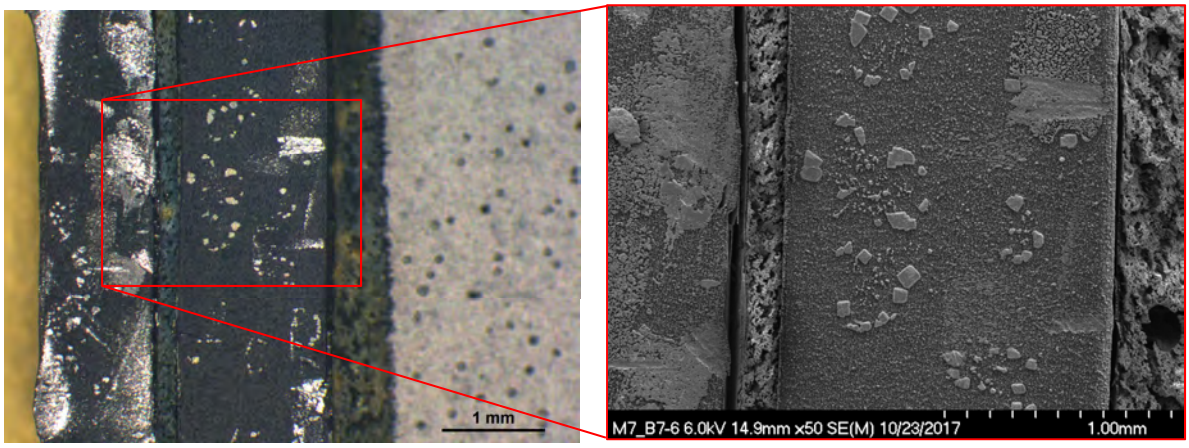

a. b.

Figure 25. Images of the edge plane HOPG after salt removal: a). Optical microscope image, and b). Electron microscope image.

Figure 26 provides an SEM image taken at a 0° tilt of the edge plane HOPG sample at a salt protected area. Figures 27a-f provides SEM images taken at 40° tilt showing three different salt protected buttes. Figures 27a, 27c and 27e show lower magnification imaged of the buttes and Figures 27c, 27 d and 27f are higher magnification images of the edge of the corresponding buttes. The erosion depth (d) measurements were obtained from SEM images such as those provided in Figures 27b, 27d and 27f. The E_y of the edge plane HOPG was based on eight different measurements and was determined to be $5.38 \pm 0.90 \times 10^{-25}$ cm^3/atom.

Figures 28a-d and Figure 29 shows the erosion texture of the HOPG edge plane. The texture is more typical of AO erosion in that there are left-standing cones. But, this material has a unique texture appearance. Figure 28a, Figure 28c and Figure 29 shows that the texture has a "directionality" to it. The cones appear to be elongated parallelograms in cross section and oriented in parallel to the graphite planes. This may be due to the differences in E_y between the basal plane and edge planes. The texture height (A) to actual erosion depth (D) ratio of the edge plane HOPG was based on eight different measurements and was determined to be 0.557.

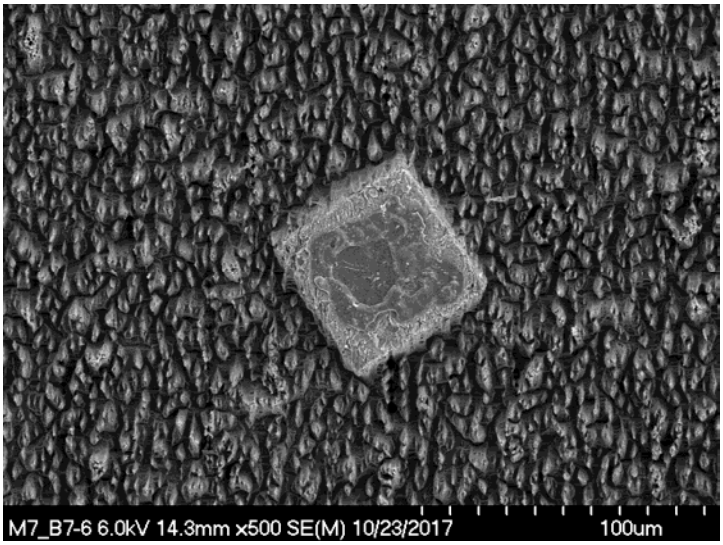

Figure 26. SEM image taken at 0° tilt of the edge plane HOPG sample at a salt protected area.

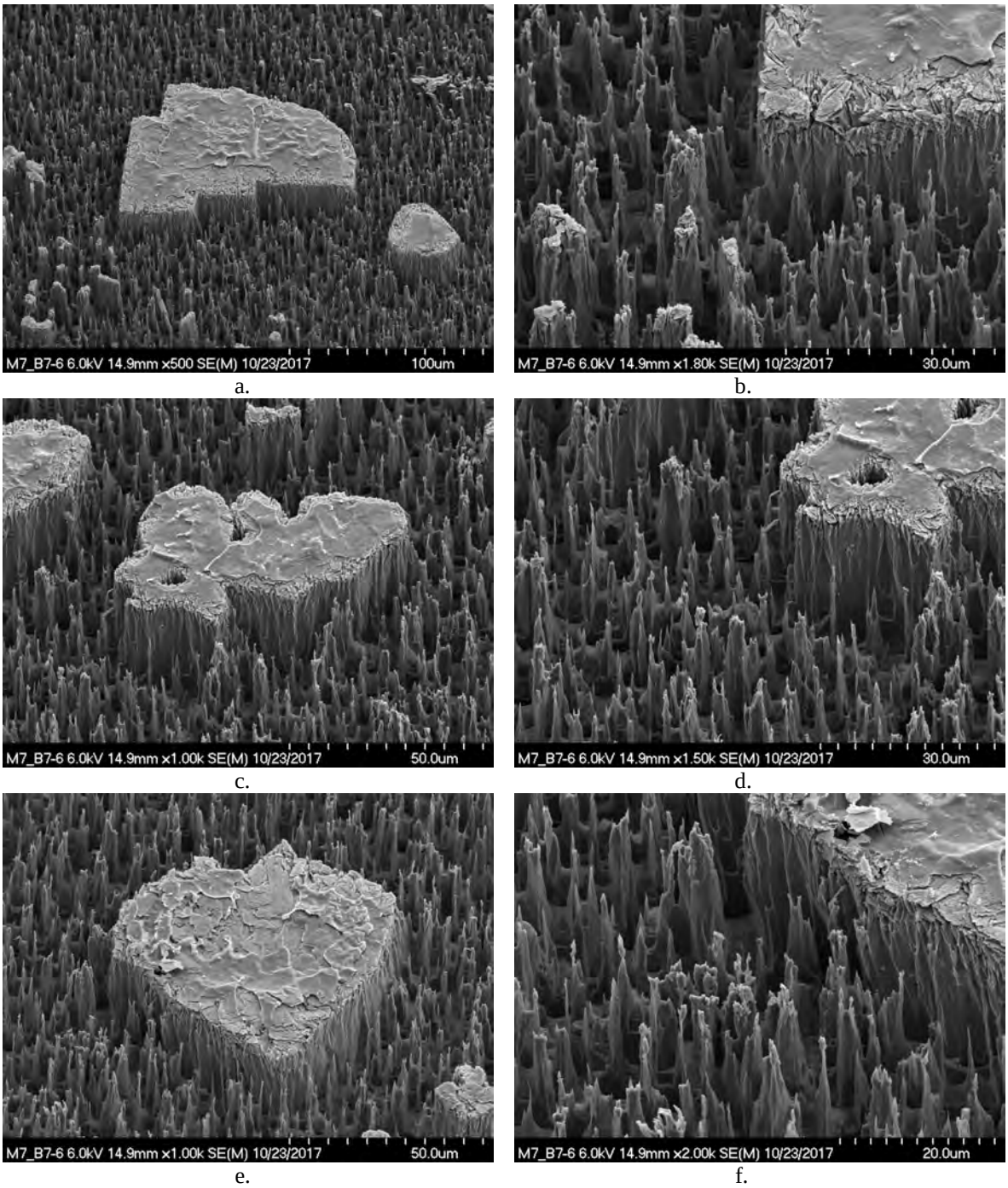

Figure 27. SEM images at 40° tilt of protected buttes on the edge plane HOPG: a). 500X magnification of Butte 1, b). 1.8kX magnification of Butte 1.), c). 1kX magnification Butte 2, d). 1.5kX magnification of Butte 2, e). 1kX magnification of heart shaped Butte 3, and f). 2kX magnification Butte 3.

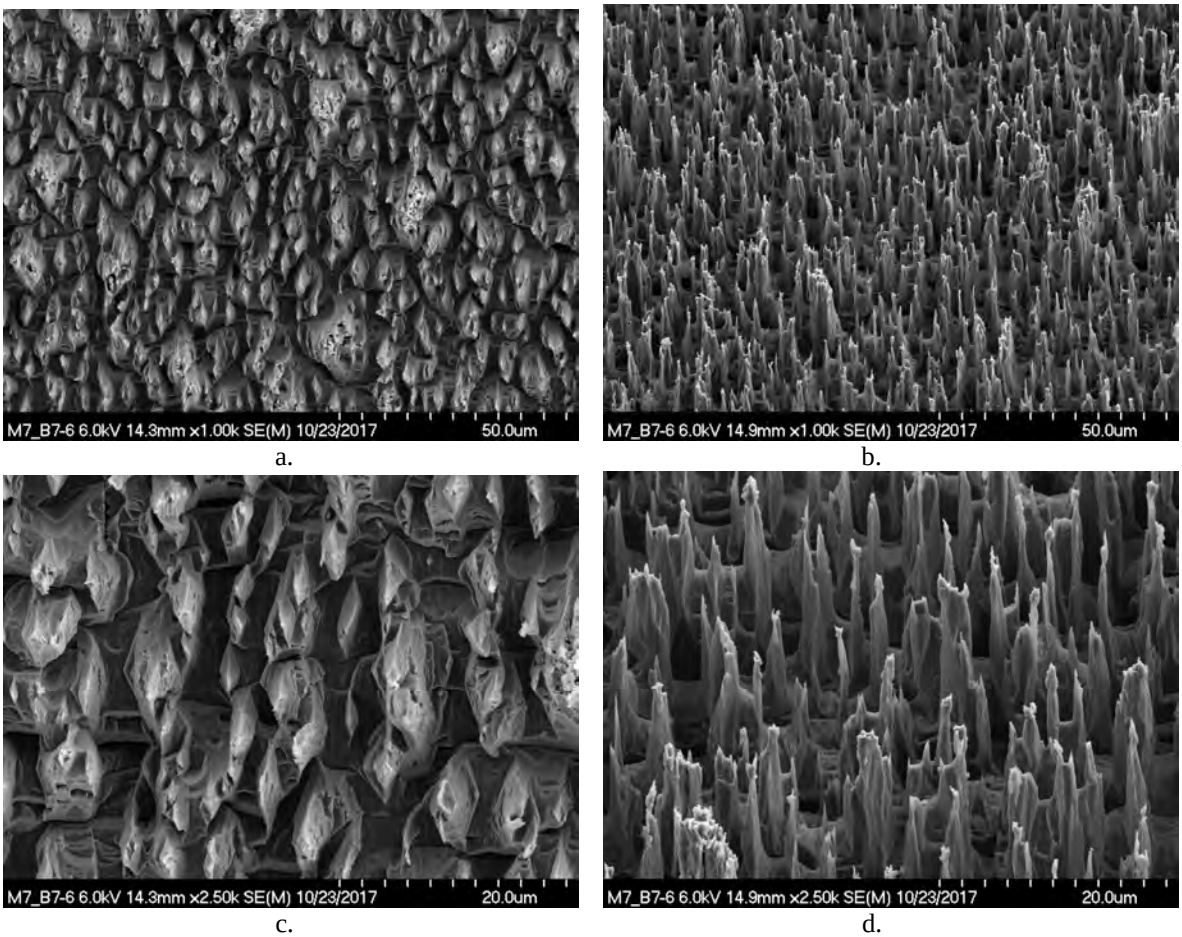

Figure 28. SEM images (0° tilt and 40° tilt) of the AO erosion texture of the basal plane HOPG: a). 1kX magnification at 0° tilt, b). 1kX magnification at 40° tilt (same area as 28a), c). 2.5kX magnification at 0° tilt, and d). 2.5kX magnification at 40° tilt (same area as 28c).

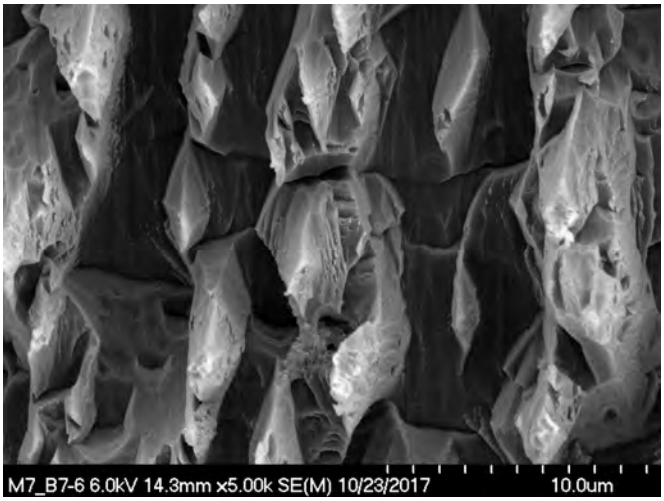

Figure 29. SEM image at 5kX magnification and 0° tilt of the AO erosion texture of the edge plane HOPG.

Summary and Conclusions

The MISSE 7 Polymers Experiment was successfully flown on the exterior of the ISS, and retrieved for post-flight analyses after 1.49 years of space exposure. As part of the experiment, a sample containing Class 2A diamond (100 plane) and highly oriented pyrolytic graphite (HOPG, basal and edge planes) were exposed to ram AO and characterized for erosion. The materials were salt-sprayed prior to flight to provide isolated AO protection. The E_y of the different materials were determined through post-flight SEM recession depth measurements.

The MISSE 7 ram samples received an AO fluence of 4.22×10^{21} atoms/cm^2 and the solar exposure was 2,400 ESH. The post-flight analyses indicated that diamond erodes, but with a very low E_y of $1.58 \pm 0.40 \times 10^{-26}$ cm^3/atom. The texture height to erosion depth ratio was determined to be 0.879, with prominent left-standing erosion cones. The different HOPG planes experienced significantly different levels of erosion. The HOPG basal plane had an E_y of $1.05 \pm 0.08 \times 10^{-24}$ cm^3/atom, while the edge plane had a lower E_y of only $5.38 \pm 0.90 \times 10^{-25}$ cm^3/atom. Thus, the basal plane HOPG eroded 2X as quickly as the edge plane. Prior MISSE 2 flight data indicated that regular PG has an E_y of $4.15 \pm 0.45 \times 10^{-25}$ cm^3/atom, which is slightly lower than the edge plane HOPG E_y. The ratio of texture height to erosion depth for the basal plane was very low (0.016) and typical AO erosion cones were not present even though the material eroded significantly. The edge plane HOPG did develop directional erosion cones and the ratio of texture height to erosion depth was 0.557. The cross-section of the cones resembled elongated parallelograms with longer sections parallel to the edge planes possibly due to the anisotropy of the E_y in the edge versus basal planes. These results confirm that Class II diamond does erode with AO exposure and documents the difference in erosion between basal and edge planes of HOPG.

References

1. Dickerson, R.E.; Gray, H.B.; Haight, G.P. (1979). *Chemical Principles 3rd Edition*. Menlo Park, CA: Benjamin Cummings Publishing Co. Inc. p. 457.
2. NASA Technical Handbook, Spacecraft Polymers Atomic Oxygen Durability Handbook (NASA-HDBK-6024), June 2014. Authored by K. K. de Groh, B. A. Banks and C. E. McCarthy.
3. NASA-TM-X-74335, U.S. Standard Atmosphere 1976.
4. Gregory, J.C. (November 10-11, 1986). "Interaction of Hyperthermal Atoms on Surfaces in Orbit: The University of Alabama Experiment." In David E. Brinza, Ed., *Proceedings of the NASA Workshop on Atomic Oxygen Effects, Nov. 10-11, 1986*. JPL 87-14, pp. 29-30.
5. Dever, J. A., "Low Earth Orbital Atomic Oxygen and Ultraviolet Radiation Effects on Polymers," NASA TM 103711, February 1991.
6. Dever, J.; Banks, B.; de Groh, K.; Miller, S. (2005). "Degradation of Spacecraft Materials." In Myer Kutz, Ed., *Handbook of Environmental Degradation of Materials*. 465-501. Norwich, NY: William Andrew Publishing.
7. O'Neal, R.L.; Levine, A.S.; Kiser, C.C. (1996). *Photographic Survey of the LDEF Mission*. NASA SP-531. NASA LaRC: Hampton, VA.

8. de Groh, K.K. and Banks, B.A. (July-August 1994). “Atomic Oxygen Undercutting of Long Duration Exposure Facility Aluminized-Kapton Multilayer Insulation.” *Journal of Spacecraft and Rockets*. Vol. 31, No. 4, pp. 656-664.
9. de Groh, K. K., Banks, B. A., Dever, J. A., Jaworske, K. J., Miller, S. K., Sechkar, E. A. and Panko, S. R., “NASA Glenn Research Center’s Materials International Space Station Experiments (MISSE 1-7),” Proceedings of the International Symposium on “SM/MPAC&SEED Experiment,” Tsukuba, Japan, March 10-11, 2008, JAXA-SP-08-015E, March 2009, pp. 91 – 119; also NASA TM-2008-215482, December 2008.
10. Banks, B.A., Mirtich, M.J., Rutledge, S.K. and Swec, D.M. (1985). “Sputtered Coatings for Protection of Spacecraft Polymers.” *Thin Solid Films*. Vol. 127, pp. 107-114.
11. Visentine, J.T., Leger, L.J., Kuminecz, J.F, and Spiker, I.K. (1985). *STS-8 Atomic Oxygen Effects Experiment*. Paper AIAA-85-0415 presented at the AIAA 23rd Aerospace Sciences Meeting. Reno, NV.
12. Koontz, S.L., Leger, L.J., Visentine, J.T., Hunton, D.E., Cross, J.B., and Hakes, C.L. (May-June 1995). “EOIM-III Mass Spectrometry and Polymer Chemistry: STS 46, July-August 1992.” *Journal of Spacecraft and Rockets*. Vol. 32, No. 3, pp. 483-495
13. Silverman, E.M. (August 1995). *Space Environmental Effects on Spacecraft: LEO Materials Selection Guide*. NASA CR-4661, Part 1. NASA MSFC: Huntsville, AL.
14. 2000 ASTM Standard Extraterrestrial Spectrum Reference E-490-00 2000 (http://rrede.nrel.gov/solar/sectra/AMO).
15. de Groh, K. K. (2010). Materials Spaceflight Experiments, in Encyclopedia of Aerospace Engineering, R. Blockley and W. Shyy (eds). John Wiley & Sons Ltd, Chichester, UK, pp 2535-2552.
16. de Groh, K. K. Banks, B. A. McCarthy, C. E. Rucker, R. N. Roberts L. M. and Berger, L. A., “MISSE 2 PEACE Polymers Atomic Oxygen Erosion Experiment on the International Space Station,” *High Performance Polymers* 20 (2008) 388-409.
17. de Groh, K. K., Banks, B. B., Mitchell, G. G., Yi, G. T., Guo, A., Ashmead, C. C., Roberts, L. M., McCarthy, C. E. and Sechkar, E. A., “MISSE 6 Stressed Polymers Experiment Atomic Oxygen Erosion Data,” Proceedings of the ‘12th International Symposium on Materials in the Space Environment (ISMSE 12)’, Noordwijk, The Netherlands (ESA SP-705, February 2013); also NASA TM-2013-217847.
18. Yi, G. T., de Groh, K. K., Banks, B. A., Haloua, A., Imka, E. C. and Mitchell, G. G. (2013). “Overview of the MISSE 7 Polymers and Zenith Polymers Experiments After 1.5 Years of Space Exposure,” Proceedings of the ‘12th International Symposium on Materials in the Space Environment (ISMSE 12)’, Noordwijk, The Netherlands (ESA SP-705, February 2013); also NASA TM-2013-217848.
19. de Groh, K. K., Banks, B. A., Yi, G. T., Haloua, A., Imka, E. C., Mitchell, G. G., Asmar, O. C., Leneghan, H. A. and Sechkar, E. A., “Erosion Results of the MISSE 7 Polymers Experiment and Zenith Polymers Experiment After 1.5 Years of Space Exposure,” NASA TM-2016-219167 (December 2016).
20. de Groh, K. K., Banks, B.A., Asmar, O. C., Yi, G. T., Mitchell, G. G., Guo, A. and Sechkar, E. A., “Erosion Results of the MISSE 8 Polymers Experiment After 2 Years of Space Exposure on the International Space Station,” NASA-TM-2017-219445 (February 2017).
21. de Groh, K. K, Perry, B. A. and Banks, B. A., “Effect of 1.5 Years of Space Exposure on Tensile Properties of Teflon,” Journal of Spacecraft and Rockets, Vol. 53, No. 6, November-December 2016, 1002-1011.

22. de Groh, K. K. Banks, B. A. Clark, G. W. Hammerstrom, A. M. Youngstrom, E. E. Kaminski, C. Fine E. S. and Marx, L. M., “A Sensitive Technique Using Atomic Force Microscopy to Measure the Low Earth Orbit Atomic Oxygen Erosion of Polymers,” presented at the Poly Millennial 2000 Conference, Kona, HI, December 9-13, 2000; NASA TM-2001-211346, December 2001.
23. de Groh, K. K., Banks, B. A. and Demko, R., “Techniques for Measuring Low Earth Orbital Atomic Oxygen Erosion of Polymers,” Proceedings of the SAMPE 2002 Conference, Long Beach, CA May 6-10, 2002, pp. 1279-1292; also NASA TM-2002-211479, March 2002.
24. Finckenor, M. M., Moore, C., Norwood, J. K., Henrie, B. and de Groh, K. “Estimated Environmental Exposures for MISSE-7B” Proceedings of the National Space and Missile Materials Symposium, Tampa, FL, June 2012.
25. Finckenor, M. M. (NASA Marshall Space Flight Center), personal communication, November 2012.
26. Banks, B., Rutledge, S. and Cales, M., “NASA Lewis Research Center EOIM-III Preliminary Results, Proceedings of the EOIM-III-3, BMDO Experiment Workshop, 1993, p. 399-442.